2010
Distinguished Teacher-Scholar Lecturer Series

Coastal Carolina University

Coastal Carolina University Distinguished Teacher-Scholar Lecturer Series

presents

Varavut Limpasuvan, Ph.D.

Professor of Applied Physics
College of Natural and Applied Sciences

"Diagnosing the beating heart of our atmosphere: a puzzle for future generations"

February 2010

Coastal Carolina University

Distinguished Teacher-Scholar Lecturer Series

The intent of the Distinguished Teacher Scholar Lecturer Series is to recognize annually a Coastal Carolina University faculty member who has distinguished himself or herself as a teacher, scholar and communicator. The awardee is an individual who embodies the University's teacher-scholar ideal of searching for and transmitting knowledge through critical inquiry and teaching in his or her discipline and who supports and appreciates critical inquiry and teaching in the other disciplines of the University. The Committee that recommends selection of the awardee is unique in that it comprises faculty members and representatives from the student body, administration and community.

The Distinguished Teacher-Scholar Lecturer Series
is made possible through the generous support of

Horry Telephone Cooperative, Inc.

Coastal Carolina University
Distinguished Teacher-Scholar Lecturer Series

Diagnosing the beating heart of our atmosphere: a puzzle for future generations

Varavut Limpasuvan, Ph.D.

Professor of Applied Physics, College of Natural and Applied Sciences
Coastal Carolina University

As concerns and debates grow over global climate change, scientists forge ahead toward grasping a better understanding of climate variability. In the atmosphere (an integral component of our climate system), research efforts are unraveling its fundamental global pattern that accounts for much of the changing wintertime meteorological conditions. As the "heart" of our atmosphere, this pattern beats in time but becomes arrhythmic in association with unusual atmospheric occurrences 30,000 feet above ground. To date, our limited knowledge of the atmosphere at these lofty heights and computational constraints make the diagnosis of this heart condition difficult and uncertain. With rapid development in technology that will allow us to better observe and simulate the atmosphere, this difficulty, which clouds our ability to assess future climate change, may be overcome by future generations.

I. Introduction

To a great extent, the weather dictates how we conduct our daily lives. Its importance is underscored in the media (e.g. newspapers, television, and the Internet) where we can easily locate a myriad of weather predictions and up-to-the-*second* meteorological conditions where we live. In examining the weather conditions (like rains, temperature, and winds) over an entire season or longer timescale, we also realize that patterns of these averaged meteorological conditions (referred to as the "climate") play fundamental roles in shaping the natural ecosystems, as well as our economies and cultures that intimately depend on them. Like the varying weather pattern, changes in the climate (on local or global scales) are crucial to our survival.

Indeed, global climate change is an issue of high international interest presently. As exemplified by the recent Copenhagen Climate Summit (December 2009), various nations and world leaders are collectively attempting to arrive at agreeable solutions to mitigate the effects of climate change while sustaining a healthy global economy. Even though climate changes can be evident in the alterations of rainfall patterns (promoting floods or droughts), humidity, and sea level, one particular aspect of global climate change commanding much intense scrutiny is "global warming" – the rising global temperature trend. The Third Assessment Report (TAR) by the Intergovernmental Panel on Climate Change (IPCC) predicts that a global temperature change of 1.4-5.8°C will occur due to global warming from 1990-2100 [*IPCC TAR*, 2001]. Figure 1 shows the IPCC prediction of global warming (relative to the global average temperature in 2000) under the "business as usual" scenario which assumes no attempts to address global warming. This scenario is characterized "by a politically and socially diverse world that exhibits sustained economic growth but does not address the inequities between rich and poor nations." Reports such as this IPCC assessment study offer important guidelines to formulate future policies and assist in our decision making process.

The projected warming trends shown in Figure 1 are derived from numerical climate system models developed at various independent scientific centers around the world. Based on highly advanced computer simulations, these models integrate the atmospheric and oceanic circulation with other relevant climate system components (like sea

ice and land characteristics) using available observations. While reflecting the level of our current understanding of the climate system, these models also reveal uncertainties in our knowledge, and each model addresses these shortcomings in its own unique ways. Despite a general agreement of the increasing global temperature trend, we clearly see that in year 2100 the predicted temperatures have a significantly broad range of nearly 2.5°C due in large part to these uncertainties.

As one would suspect, our understanding of the climate system is obviously far from complete. In the atmosphere (an essential component of the climate system), we are just beginning to learn more about an atmospheric region between 10-90 kilometers (km) or ~32,000-292,000 feet (ft) that has been much ignored in the past and has been referred to, jokingly, as the "ignorosphere" [*Andrews et al.*, 1987]. Officially, the lower part of the ignorosphere (below 50 km) is known as the "stratosphere" while the upper portion (above 50 km) is called the "mesosphere". Past lack of interest is rooted in the fact that, as surface dwellers, only the air near the surface (the "troposphere") seems to have direct relevance to us and that the thin atmosphere above 10 km is generally difficult to observe. Nevertheless, the question of how air, matter and circulation at these high altitudes can influence the climate system is just now coming to light [e.g. *Hartmann et al.*, 2000]. As such, these climate system models are continually being extended vertically from the ground to account for the atmosphere at these lofty heights.

Furthermore, we are beginning to unveil the natural behavior of the atmospheric component of the climate system. Analyses of growing global observations and model results suggest that the global atmosphere exhibits a natural behavior (called the "atmospheric climate mode") irrespective of anomalous external influences that can affect the climate system (e.g. increasing carbon dioxide or sulfate aerosols, volcanic activities, and solar activity). This atmospheric mode appears as a very simple global meteorological pattern that oscillates in time. Its appearance is quite remarkable given the chaotic and incessant nature of the fluid atmosphere. By better understanding this natural atmospheric mode, we can effectively analyze how the integrated climate system may be changing in response to external influences and anthropogenic effects.

To this end, this paper highlights new understanding of our atmosphere from the climate context. Focusing on the Northern Hemisphere wintertime climate (December to March), we discuss the natural atmospheric mode of climate variability and how we derive at its pattern and time evolution. To facilitate this discussion, we first illustrate the basic climate state of the wintertime atmosphere and then explain how this natural mode embodies nearly a *third* of all departures of the atmospheric state from climatology. A remarkable occurrence predominantly in the stratosphere is presented as part of the drastic breakdown of the fluid circulation in the ignorosphere. We offer evidence on how the demise of this circulation influences the phase of the naturally occurring atmospheric climate mode [*Hartmann and Limpasuvan*, 2004]. We underline the importance of atmospheric wave disturbances and how they affect the overall atmospheric circulation.

As a naturally fluctuating pattern that evolves in time, this atmospheric mode of climate variability can be thought of as the "heart" of our entire atmosphere. The changing phase of this pattern is like the expansion and contraction of the human heart. The alternating phases of the mode reflect the changes in our weather pattern and the overall tendencies of our atmosphere mirror how the various parts of our bodies (e.g. lungs and chest cavity) work in concert with our very own heart. As we shall see, the beating of this atmospheric mode is irregular and non-predictable. The drastic events in the circulation break-down in the stratosphere and mesosphere can provide sharp "jolts" to the beating atmospheric "heart", making it arrhythmic with respect to its normal state.

To keep focus on the science, we stay clear of the heated debate on whether global warming is actually happening or if the warming is anthropogenically induced. Instead, we highlight the shortcomings of present atmospheric components of the climate system models that are designed to help us assess future climate changes, as noted in Figure 1. We discuss how scientists are addressing this deficiency. We note that while these climate system models can emulate the atmospheric climate mode, they have difficulties producing the drastic events in the ignorosphere.

Therefore, our ability to diagnose the anomalous conditions of the atmospheric beating heart is limited and uncertain. However, given the rapid development of computing technology and engineering advances that will allow us to better observe and model the atmosphere, this problem has a potentially attainable solution that future generations will have the unenviable task of deriving.

Unless noted otherwise, illustrations in the paper are constructed by the author using analyzed data from various sources based on the latest data processing techniques that integrate available observations, numerical computer models, and our knowledge of physics and chemistry. The first analyzed data set is from the National Aeronautics and Space Administration (NASA) Goddard Earth Observing System Model, Version 5 (GEOS-5) product. Covering the time period of 2003-2009, this data set integrates the GEOS-5 atmospheric Global Climate Model (GEOS-5 GCM) with the available observations from various NASA satellite platforms [*Bloom et al.*, 2005]. The other analyzed data set comes from the National Center for the Environmental Prediction and National Center for Atmosphere Research (NCEP/NCAR) re-analyses product from 1958-2001 [*Kalnay et al.*, 1996]. The initial NCEP/NCAR data is derived similarly to the GEOS-5 product; however, it is periodically re-processed as more observations become available. In addition to these analyzed data set, we examine data retrieved directly from the NASA Earth Observing Satellite-AURA Microwave Limb Sounder (MLS) instruments from 2003-2009 [*Waters et al.*, 2006; *Schwartz et al.*, 2006]. Scanned vertically along the polar orbiting satellite path, this data measures the microwave electromagnetic wave signal emitted by various atmospheric constitutions to infer atmospheric temperatures, from which we derive winds. Finally, we utilize a newly developed weather model on a global scale based on the University of Oklahoma's Advanced Regional Prediction Systems (ARPS) [*Xue et al.*, 2003]. This development effort has been conducted at Coastal Carolina University by the author and undergraduate research assistants. From this model, we illustrate detailed features of the atmosphere not present in the climate models or most weather models. As we shall see, these features may hold the keys to improving climate models and their ability to assess future climate changes.

II. The Basic Climatology: The Jet Stream and the Polar Vortex

Our local impression of the atmosphere is that it is highly variable. The weather could be pleasant and sunny one winter day, cloudy and stormy the next. If we examine our atmosphere from a global perspective, we see that the local changes in the weather we experience are really just part of the ever changing flow pattern circulating around the globe. Figure 2 shows an example of the circulation of our atmosphere at an instant on Christmas day 2005 and 11 January 2009. For each day (in each column), the top, middle, and bottom figures show the atmospheric flow at 5, 20, and 30 km above ground, respectively. At a given altitude, the air motion tends to flow parallel to the illustrated contour lines in the direction of the overlaid arrows. The winds are strongest (longest arrows) where the contour lines are closely packed together. The background colors indicate the air temperature (with the temperature scale shown by the color bar). Blue indicates cooler air and red the warmer air.

From these maps, we see that the atmospheric flows are generally directed from east to west and in a counterclockwise sense with the North Pole as the center. That is, the wintertime atmospheric motion is predominantly governed by a *circumpolar* flow. Between the surface and 10 km (~32,000 feet) above ground (in the atmospheric layer referred to as the "troposphere"), the circumpolar flow is associated with the Jet Stream. Above 10 km, in the atmospheric layer referred to as the "stratosphere", the circumpolar flow is referred to as the Polar Vortex. As illustrated in color temperature map, the streaming circumpolar flow tends to divide the colder polar air masses from low latitude regions. Recall that the stratosphere is the lower portion of the ignorosphere.

Obviously, this circumpolar flow and temperature distribution fluctuate widely from day to day, especially in the troposphere. Just note the differences in the illustrations of each column in Figure 2. To characterize the flow for a typical wintertime day, we examine the long-term average (or climatology) of wind and temperature. Figure 3 shows the averaged wind strength of the Jet Stream from maps like those shown in the top row of Figure 2 for all days

from December to February in the entire 1958-2001 NCEP/NCAR data. For simplicity, we only show the strength of the climatological Jet Stream winds as line contours, with red lines indicating winds in the west-to-east direction and blue lines representing winds in the east-to-west direction. Given the absence of blue lines in the figure, we see that the climatological Jet Stream is always flowing from west-to-east and is fastest around the 30 degree North (30°N) latitude circle. For reference, this latitude ring is shown in Figure 3A as a dashed magenta circle. The local maximum wind of around 30 m/s appears over the Atlantic Ocean and a relatively stronger wind (about 50 m/s) resides over the Pacific Ocean.

Superimposed on Figure 3A are areas of intense storm activities in blue shading. These heavy precipitation activities tend to move from west-to-east over the ocean sectors, decaying as they approach Northwestern America and Northern Europe. Given this pattern, it is not surprising that the wintertime climate conditions over Seattle and Dublin (Ireland) are similar (that is, cold and wet). We see that storm areas at the 5 km level are just slightly eastward of the strong wind centers. Near-surface weather systems are generally westward of the overlying storm systems [*Holton*, 1972]. As such, the Jet Stream is the governor of our weather patterns: strong weather systems tend to follow the strong Jet Stream winds. Meteorologists therefore rely on the daily Jet Stream pattern to help guide their forecasts.

Because of the interaction with the Earth's surface, the climatological near-surface winds are more complex (see arrows in Figure 3B). Nonetheless, strong winds (longest arrows) are generally found over the oceans similar to the Jet Stream, with wind speed faster than 10 m/s. The near-surface winds tend to organize into counterclockwise gyres near North Atlantic and North Pacific Ocean and collocate with low sea level pressure (SLP) centers (as marked by "L" in the illustration). Physically, SLP (shown as line contours) represents the amount of atmospheric weight above any given location on the Earth's surface per unit area. For example, a 1,010 hecto-Pascal (hPa) SLP value means that, in an area of 1 square foot, the overlying atmospheric weight pressing down on that surface area is about 2,000 pounds of force. A dominant high pressure center ("H") persists over the Eurasian region with predominantly clockwise surface wind gyres.

From time-averaged maps like Figure 3, we note that the climatological values *away from the ground surface* tend to align (on the first order) with the latitude rings. For example, if we transverse along the dashed magenta circle in Figure 3A, the climatological Jet Stream strength does not vary greatly. As such, to obtain the distribution of the climatological field as a function of altitude, we can compute the averaged wind strength values along each latitude circle. We can then repeat this computational process for all altitude levels over the entire winter. The same algorithm can be applied to the temperature distribution.

Figure 4 illustrates the result of this calculation as a latitude-altitude distribution of the climatological temperature and wind strength. In the Northern Hemisphere (which experiences winter during December to February), the strong west-to-east winds (red line contours) are evident at nearly all levels from 20°N-90°N (see Figure 4B). Consistent with Figures 2 and 3, the Jet Stream is climatologically centered near 30°N latitude circle and peaks at about 40 m/s near the "tropopause" (green dashed line) which marks the boundary between the troposphere and the stratosphere. The bottom portion of the Polar Vortex is climatologically located near 70°N with peak speed of about 30 m/s. In the upper stratosphere (say, around 45 km), the Polar Vortex can exceed 50 m/s (not shown). At any given latitude, the increasing wind strength with height is linked to the temperature distribution in which relatively colder air is found to the north. This is noted in Figure 4A as "W" and "C" for warm and cold, respectively. As such, regions of strong winds (i.e. the cores of the Jet Stream and the Polar Vortex) mark the division between the cold polar air masses from the warmer air at lower latitudes. We noted this division in Figure 2, where the blue color temperatures are confined by the evolving Jet Stream and the Polar Vortex.

To this end, we have introduced the key components in our atmosphere needed to further our discussion. In focusing on the wintertime conditions (between December and March) in the Northern Hemisphere, we have

illustrated the presence of strong circumpolar flows that vary daily. We differentiate between the Jet Stream and the Polar Vortex as the flow that takes place predominantly in the troposphere and stratosphere, respectively. The associated strong streaming winds mark the boundary between the cold polar air masses from the rest of the globe. We further characterize these flows and other important atmospheric quantities like sea level pressure and temperature by simple averaging in time to obtain the winter climatology. In doing so, we see that the climatological position of the Jet Stream is intimately linked to areas of severe storm and weather activities. We see also that the sea level pressure distribution tends to become geographically organized. In addition to time averaging, we can perform an average of various meteorological values at each latitude circle. In doing so, we can derive at latitude-altitude distribution maps that help illustrate the global structure of the atmosphere as it varies in height.

III. The Fluctuating Circumpolar Flow: Atmospheric Climate Mode

As seen in Figure 2, the atmospheric flow can be quite complex and highly variable. If possible, we'd like to get a sense of how the atmospheric state on a given winter day differs from the climatological state. For example, based on the data gathered by the South Carolina State Climatology Office from 1971-2000, we expect Charleston to have an average December temperature of 61°F. However, let us suppose that the actual averaged December temperature of the year 2015 in Charleston turns out to be a scorching 100°F. In that case, we would like to have some ideas why such temperature anomalies exist.

Recent research efforts are attempting to characterize how the atmosphere fluctuates with respect to climatology using the long-term SLP data [*Thompson and Wallace*, 1998]. Based on the SLP climatology shown in Figure 3, the SLP departures from that climatological state are defined as SLP anomalies. Using statistical tools called the *Empirical Orthogonal Function* (EOF) analysis, the spatial structure of the predominant modes of these anomalies (i.e. "leading mode of variability") can be determined along with an associated (non-dimensional) time series that describes how this structure changes. Moreover, the technique also objectively reveals the extent to which this mode accounts for all of the departures from climatology. Since SLP is a measure of the overlying atmospheric weight per unit area, it serves as a great representation of the atmosphere as a whole from the surface to the very top of our atmosphere. Variations in the circumpolar winds are related to changes in atmospheric weight since they embody the movement of air matter from one region to another.

Figure 5 shows the (normalized) time series of leading mode and the spatial structure of the leading SLP mode of variability when the time series is positive and has a unit amplitude. The contour values represent the amount of SLP departure from its climatological values shown in Figure 3B, with the blue lines indicating values below climatology and red above climatology. The black line shows where the SLP values are essentially identical to climatology. In general, when the index is positive, the spatial structure indicates that SLP is below its climatological values over much of the polar region (i.e. blue negative contours) and above its climatological values in the periphery. The amount of SLP departure depends on the amplitude of the index. If the index is one, then the departure value is given as shown in the illustration. When the index is negative, the SLP distribution is the opposite of what is shown (i.e. above climatological values over the polar region). For example, on 18 December 1925 when the time series is one, the SLP values over Iceland for that day will be roughly 15 hPa below its climatological values. In 1938, when the time series is negative and one on that same day, the Iceland SLP value will be 15 hPa below its climatological values.

Overall, as the time series varies in time, we see that this leading mode of SLP variability describes a "see-saw" behavior of the SLP distribution in time with the "fulcrum" represented by the black contour (where the SLP anomaly is zero). By superimposing the Arctic Circle (or the 60°N latitude band) as a dashed magenta ring on Figure 5, we note that this fulcrum nearly parallels the Arctic boundary. As such, this mode is referred to as the *Northern Hemisphere Annular Mode* (NAM) since the fulcrum of the see-saw is ring-like (i.e. "annular" in shape). The associated

time series is referred to as the NAM index. When the index is positive and the polar SLP is anomalously low, the NAM is said to be in the high phase. When the index is negative, the NAM is in its low phase. Remarkably, the NAM mode accounts for nearly as much as 35 percent of all departures from climatology [*Thompson and Wallace*, 2001].

Recall that SLP indicates the amount of atmospheric weight per unit area at the surface. From Figure 5, we see that the overlaying atmospheric content tends to fluctuate across the Arctic Circle. When the index is positive (or high NAM phase), with anomalously low SLP over the polar region, most of the atmospheric weight is distributed more toward the tropics. Given that nearly 80% of the atmospheric mass resides in the troposphere [*Wallace and Hobbs*, 2006], the NAM essentially captures the fluctuation in the troposphere conditions. Clearly, the time series has no obvious periodicity and this mode is believed to be a manifestation of the natural (resonant) behavior of the atmosphere [*Hartmann et al.*, 2000; *Limpasuvan and Hartmann*, 2000]. As such, there is no clear-cut reason for the cause of the NAM other than that it is the natural response to various random disturbances in the atmosphere. In the wintertime Southern Hemisphere (June-August), an analogous atmospheric climate mode exists in the form of the Southern Hemisphere Annular Mode (SAM) [e.g. *Gillett et al.*, 2006]. In fact, any rotating fluids surrounding a sphere (like our atmosphere for example) should exhibit a ring-like (annular) mode of variability like the NAM.

We can correlate the NAM index with various observed atmospheric quantities such as precipitation, the extent of the polar vortex, and the position of the storm system associated with the Jet Stream [*Thompson and Wallace*, 2001]. Figure 6 summarizes the changes in the atmosphere as the NAM fluctuates from the low phase (on the left) and the high phase (on the right). During the high phase, the location of the Jet Stream over the Atlantic tends to be more northward. This configuration brings more severe storms and heavy rainfall to Northern Europe. However, conditions in the Mediterranean are generally dry and sunny [*Orsolini and Limpasuvan*, 2001]. Less cold outbreaks and snowfall occur over Eastern United States. In the stratosphere, the Polar Vortex tends to also be stronger with intense circumpolar winds. When the low NAM phase occurs, the Jet Stream over the Atlantic Ocean tends to drift southward leading to wetter and cloudier conditions over Southern Europe. Northern Europe experiences dry but very cold conditions while the Eastern United States braces for a higher probability of heavy snowfall. The Polar Vortex tends to be broader and less intense. Interestingly, the trade winds near the tropical regions also exhibit some response to the changing NAM phase.

IV. The Stratospheric Disturbance: Polar Vortex Breaking

During certain winters, the Polar Vortex reverses in direction and polar atmosphere becomes much warmer than climatology. We can see this unusual warming event in recent satellite observations from the MLS instrument aboard NASA's Aura spacecraft. The left column of Figure 7 illustrates the strength of the circumpolar winds averaged at the 70°N latitude circle during the wintertime period. Color scales from yellow to magenta indicate increasing strength of the wind flowing to the east (i.e. counterclockwise flow as shown in Figure 2) and a strong circumpolar flow. Color scales from green to purple indicate increasing strength of the wind flowing to the west (i.e. clockwise flow) and a weak circumpolar flow. Within a given winter season, while the circumpolar flow is predominantly eastward, the flow strength is highly variable. In the stratospheric layer (between 10-50 km as marked by the dashed, black horizontal lines), the Polar Vortex sustains winds around 40-70 m/s. The right column of Figure 7 shows the corresponding temperature averaged at the 70°N latitude circle. Warmer areas are noted in red tone and cooler areas in blue tone. Around the 55-km level, we note the relatively warm air layer called the "stratopause" that marks the boundary between the stratosphere and the mesosphere. Like the noted circumpolar wind strength, the temperature distribution is also variable during the winter.

The MLS observations show the remarkable reversal of the circumpolar flow in the stratosphere. This can be seen by the presence of the green colors in the left column with the overlaid black contours indicating where the

flow begins to reverse. The reversal period (green-blue areas) can persist for a few days up to as long as 20 days (as in the case of the 2005-06 winter). During the incipient stage of the wind reversal, we note the descent of the warm stratopause air band near 55 km. This warm descent becomes very pronounced as the wind reversal (the black contour line) appears and the polar temperature in the upper stratosphere (between 30 and 50 km) undergoes rapid warming. This coupled phenomenon of circumpolar wind reversal and rapid warming over the polar region is commonly referred to as a major "sudden stratospheric warming" (SSW) [*Andrews et al.*, 1987]. In the observed time period, two major SSWs were observed during the 2005-06 and the 2008-09 winters and are highlighted by the thick dashed rectangles in Figure 7. During these episodes, the warm layer near 50 km actually became severed (discontinuity in the yellow temperature contours) as the polar vortex recovers and the circumpolar winds begin to flow eastward again. Historically, major SSWs occur about 6 times every 10 years [*Charlton et al.*, 2007]; however, their occurrences are not periodic.

Episodes of the circumpolar wind reversal and polar warming inherent in SSWs are associated with the "breakdown" of the Polar Vortex. This breakdown process occurs as a result of a strong vortex displacement or vortex splitting. Figure 8 shows the occurrence of both types of SSWs during January of 2006 and 2009, noted in Figure 7. In the preceding meteorological conditions (on 25 December 2005 and 11 January 2009) as displayed in Figure 2, we note that Polar Vortex in the middle and upper stratosphere was very strong and extremely cold. The polar temperature dips well below 200 K and the circumpolar winds are nearly all directed in the counterclockwise sense (Figure 2). Near 30 km, the onset of the 2006 SSW is marked by a strong displacement of the cold counterclockwise vortex (noted by "L") toward Scandinavia and the development of a relatively warm clockwise vortex (right column, Figure 8) as noted by "H". During the 2009 SSW, the polar vortex is divided into two counterclockwise gyres (centered over North American and another over Northern Eurasian) with two adjacent clockwise circulations.

Regardless of the vortex conditions during SSW, at a given latitude circle in the polar region, we see that the circumpolar flow becomes predominantly from east to west as polar warming occurs. As such, from an average point of view at a polar latitude circle like 70°N as shown in Figure 8, the polar wind direction is now reversed from the conditions during 25 December 2005 and 11 January 2009 (Figure 2). Consistent with SSWs, the polar temperature on the whole has also become much warmer as we can see from the presence of reddish orange colors near the pole in Figure 8. Overall, these behaviors are consistent with the height-time evolution shown in Figure 7.

V. Understanding the Demise of the Polar Vortex

Our understanding of SSW is still far from complete. However, the key contributors to the SSW occurrence are atmospheric waves. In the ocean, we can clearly see the passage of waves of various spatial scales and speed. In the atmosphere, wave motions are essentially invisible to the naked eye although we catch glimpses of their presences in clouds. However, their presence is indeed extremely important to the whole atmosphere.

In the troposphere, the circumpolar flow is continually disturbed throughout the winter by atmospheric waves and spontaneous adjustment processes within the flow. In fact, the word "troposphere" has a Greek root word *tropos* which means "turning" or "mixing" to reflect the active movement in the atmospheric layer near the surface. Dominant wave source is linked to land-sea distribution and orography in the Northern Hemisphere. Combined with the Earth's rotational effects, heating and frictional difference between land and ocean and large-scale surface undulations help drive large-scale atmospheric disturbances commonly referred to as *Planetary Waves* [*Salby*, 1996]. With spatial scale larger than 5000 km, these waves are responsible for the meandering observed in the Jet Stream, shown in Figures 2 and 8.

Likewise, spontaneous adjustment in the troposphere can lead to wave disturbance even in the absence of topography. As the Jet Stream meanders, the north-south temperature contrasts that accompany the circumpolar

flow can become very pronounced at certain locations on the globe (marked as weather "fronts"). In the 5-km level maps of Figures 2 and 8, strong temperature contrast (or gradient) can be identified in regions where the green areas are tightly squeezed between blue (cold air) and red (warm air) regions and the black line contours are packed together. Such temperature gradient can render the atmosphere unstable, potentially causing the atmosphere to undergo adjustment processes that alleviate this situation. These processes can manifest themselves as synoptic-scale wave disturbances on spatial scales of 1500-5000 km. They are responsible for daily weather patterns and have a life span of about a week or so. In fact, the blue regions shown in Figure 3A identify the climatological location of strong *synoptic-scale* wave activities [*James*, 1994].

Unlike the active troposphere (replete with weather occurrences embedded into planetary waves), the circulation in the stratosphere is relatively calmer. The term "stratosphere" is based on the Latin word *stratum*, which means "layer" to reflect the relatively calm nature of the atmosphere above ~12 km. Nonetheless, like its tropospheric counterpart, the stratospheric circumpolar flow is continually disturbed by waves and spontaneous adjustments (as suggested in Figures 2 and 8). In fact, the very same planetary waves that bother the Jet Stream can eventually make their way into the stratosphere. However, the strong winds in the stratosphere and the temperature structure near the tropopause conspire to serve as a natural atmospheric filter that only allows planetary waves of the largest scale (above 15,000 km) to penetrate into the stratosphere [*Andrews et al.*, 1987]. The presence of large-scale planetary waves in the stratosphere are readily apparent when the Polar Vortex wobbles and becomes slightly displaced off the pole. This same natural filtering effect of the atmosphere also traps synoptic-scale wave disturbances near the tropopause [*James*, 1994].

Figure 9A shows the wintertime average propagation of planetary waves for the winter of 2008-09. The magnitude of planetary wave disturbance and its direction of propagation are given as arrows. Between 40°-80°N, we see that the waves in the atmosphere emanate upward mainly from the mid-latitude range. As they make their way across the upper region of the troposphere, much of the wave activity is trapped in the troposphere due to the aforementioned natural filtering effects of the atmospheric background conditions. As such, fewer arrows penetrate across the tropopause (marked by the lower dashed white line). Poleward of 40°N, planetary waves of largest scales eventually penetrate into the upper stratosphere. The unfilled contours show the strength of the circumpolar wind averaged about each latitude circles (similar to Figure 4B). Solid contour lines indicate winds from west-to-east, and broken lines indicate winds from east-to-west. We note that in the Southern Hemisphere (which is experiencing summer) planetary waves are also present in the troposphere. However, they are all prohibited to propagate in the summer stratosphere. The first order reason for this restriction is due to the prevailing east-to-west stratospheric winds (broken contour lines) which are opposite to the tropospheric flow. Such opposite flow direction leads to strong wind shear that prevents upward propagation of planetary waves.

The amount of planetary wave energy is proportional to the length of the arrows. We see that the energy diminishes as the waves enter the stratosphere. This energy loss reflects the exchange in the wave energy with the circumpolar flow, and the net interaction effects can lead to either the acceleration or deceleration of the background circumpolar winds. The filled contours indicate the amount of accelerative/decelerative effects of planetary waves on the winds: blue colors representing the decelerative effects and red colors the accelerative effects. We note that, since much of the atmospheric mass resides in the troposphere, a very small amount of planetary wave energy exchange is needed in the stratosphere to have the same effects as the much larger energy exchange in the lower atmosphere.

In the seasonal average (Figure 9A), we see that the presence of planetary waves in the wintertime stratosphere tend to decelerate (slow down) the polar vortex by about 10-30 m/s per day (see the small blue region around 20-50 km), so that the polar vortex on the average has a peak strength of about 50 m/s. Indeed, the presence of planetary waves helps to maintain the polar vortex strength as we saw in the climatological state shown in Figure 4. In the absence of these waves, the polar vortex would be much faster than reality. As we will elaborate further in sections below, these waves help maintain the momentum and thermal budget of the atmosphere.

Figure 9B shows the recent planetary wave activities as they propagate from the troposphere through the stratosphere during the SSW episode of January 2009. In contrast to the winter average plot shown on Figure 9A, we clearly note the tremendous growth in planetary wave activity in the troposphere and the enhanced penetration into the stratosphere. Associated with SSW onset, the Polar Vortex is now dominated by the east-to-west wind around 40-50 km between 40°-60°N (as seen by the presence of dashed contour lines). This condition is indicative of the Polar Vortex breakdown and the circumpolar wind reversal (noted in Figure 8, right column). The wind structure is indeed very different from the climatology shown in Figure 9A due to the decelerative effects of the converging wave activity in the upper portion of the stratosphere. In Figure 9B, we see a widespread deceleration (blue) region in the Northern Hemisphere stratosphere with deceleration values exceeding more than -50 m/s per day. To this end, the widely accepted explanation for SSWs is due to the anomalous propagation of the planetary waves into in the stratospheric polar region. The decelerative effects imposed by these waves cause the Polar Vortex breakdown. However, what triggers the anomalous planetary wave propagation in the first place is still very much a mystery.

VI. Polar Vortex Influence on the Jet Stream

As seen in Figure 7, incipient circumpolar wind reversal (green regions) appears to begin well above the top of the stratosphere and descend toward the tropopause (around 10 km). The warm air layer near the stratopause exhibits a similar descent. However, in some years (like the 2009 SSW event), we actually see that the wind reversal appears to reach the surface. As such, this near-surface extension of circumpolar wind reversal may provide possible influence to the Jet Stream (and ultimately our weather pattern). In going back to past data records, we see that other SSW events also appear to have strong connection to the troposphere [*Baldwin and Dunkerton*, 2001]. Hence, there are suggestions that SSWs are strongly coupled to near-surface climate [*Limpasuvan et al.*, 2004 and 2005].

To examine this connection, we first identify all SSW occurrences in the NCEP/NCAR re-analyses from 1958-2001. In all, 23 major SSW events were found. From each event, we define the SSW life cycle as an 81-day time series to capture the entire evolution of SSW as its start, matures to maximum wind reversal warming, and eventual decay. The central date of this life cycle (called day 0) corresponds to when then largest wind reversal occurs; that is, when the SSW is fully mature. With respect to that central date, we sample 40 days before (negative days) and 40 days after (positive days). We then composite all of the identified SSW life cycle to ascertain the first order behavior of the atmosphere as SSW occurs. For this algorithm, we will use wind condition at 10 hPa to define the life cycle. From Figure 7, we see that the SSW process lasts well over 20 days, so this 81-day life cycle fully captures the SSW events. We emphasize this methodology simply help us ascertain the SSW behavior from a climatological point-of-view. Individual SSW events can vary from this climatology.

Figure 10A shows the circumpolar wind strength and direction during the composite SSW life cycle. At both 32 km (~10 hPa) and 15 km (~150 hPa), we see that as SSW starts the Polar Vortex is initially weak and circumpolar wind flows in the west-to-east direction (positive value). At 30 days before day 0, the wind begins to change direction (becoming negative) which marks the onset of SSW. The reversed wind becomes stronger and peaks at day 0 as expected based on how we define the SSW life cycle. After the central date, SSW begins to recover and the reversed wind weakens. The recovery process is completed roughly 25 days after day 0.

Figure 10B shows the NAM index (as seen in Figure 5) compiled with respect to the SSW life cycle of Figure 10A. Prior to day -15, the NAM index during the developmental stage of SSW is weak and nearly zero. As such, the atmospheric mass distribution and the meteorological conditions are essentially in their climatological state. As SSW begins to mature with the approach of the central date (day 0), the NAM index rapidly becomes large in amplitude and shifts toward its low (negative) phase. The NAM remains in its strong negative phase for nearly 10 day after maturation of SSW as the wind reversal weakens. As the polar vortex recovers and SSW subsides, the NAM index lingers in the negative phase at reduced amplitude.

These results suggest that very strong anomalous events in the stratosphere like SSWs can bias the NAM, the leading mode of atmospheric climate variability. In Figure 10, we note that at least a 30-day lag is evident between the stratosphere and troposphere from the onset time of SSWs (about day -30 of the life cycle) to the peak in the negative NAM index around day 5-10. From Figure 6, we see that low NAM phase corresponds to wintertime conditions in which the Jet Stream retreats closer to the Arctic Circle. Wet and stormy condition tends to occur at higher latitude regions. Such lag suggests that variability in the stratospheric Polar Vortex yields a useful level of predictive skill for Northern Hemisphere wintertime forecast on both intraseasonal and seasonal timescales [*Hurrell et al*, 2003]. That is, if we observe changes in the Polar Vortex leading potentially to SSW, then we can improve how we make weather and climate forecast near the surface, based on the expected change in the NAM index to follow. In addition, other studies suggest that the Polar Vortex can also undergo very unusual strengthening and the associated circumpolar wind intensification can likewise influences the NAM index [*Baldwin and Dunkerton*, 2001; *Limpasuvan et al*., 2005]. ***To this end, improved knowledge of the stratosphere (and the mesosphere) is important to further our understanding of the weather and climate near the surface.*** This knowledge comes from having ample observational data and ways to model and interpret our observations.

VII. Observations and Life with Super Models

The ever-increasing numbers of observations provided by satellites and local networks of observations are continually adding to our understanding of the variability of the circumpolar flow in the troposphere and stratosphere. Obviously, given the complexity and scales of our atmosphere, there are always glaring limitations to every type of observations. Local observations (like balloon soundings or weather stations) measure local atmospheric conditions at one location at one or multiple levels. While this type of data sampling is perfect in providing localized and detailed conditions, we would need measurements at numerous places across the hemisphere to study global changes related to NAM or SSW. Even then, such measurement network may not be possible at certain places like over the ocean or where the conditions (freezing temperature or high winds) are not amenable for the instruments. Observations like those from satellites provide nearly global coverage but these observations are not instantaneous. For example, a polar orbiting satellite has to orbit the globe nearly 14 times to sample for the entire hemisphere. As such, satellite techniques always preclude rapid atmosphere variations or disturbances of smaller scales than the satellite scanning footprint. Nevertheless, improved observational techniques are being developed to better monitor the atmosphere. To date, the best way to understand the atmosphere is by combining the available observational data with numerical models. These models are mathematical tools based on our best understanding of the physics and chemistry of the atmosphere and fluid mechanics. In brief, these models divide each atmospheric domain layer into a grid. The spacing between each grid point determines the horizontal resolution of the model and the spacing between each atmospheric layer determines the vertical resolution of the model (Figure 11). The total number of grid points in the model depends on the areal size of the layer and the number of layers used in the model. For a given model domain and vertical extension, the coarseness of the model resolution determines the total number of grid points. Each grid point holds the values of at least 10 atmospheric variables. These models provide prognostics of future atmospheric states in a predetermined time step (temporal resolution). In all, the domain size, the vertical extent of the model, as well as the model resolution dictate how much computing resources are needed to run the model.

Weather forecast models can provide us with general views of the tropospheric evolution due to planetary waves and synoptic-scale disturbances up to 7-10 days in advance. For regions like the continental United States, these forecast models tend to have a horizontal spatial resolution of 10 to 20 km. That is, predictions of atmospheric variables (like temperature, SLP, and winds) are provided by these models at locations on the map every 10-20 km (~6-12 miles) apart. Given the readily available computing resources, these weather models extend vertically just above the tropopause (~20 km) in order to be operationally cost-effective. That is, with this physical set-up, the models can provide forecast results in a reasonable amount of time. To improve forecast, higher resolution

(say 5-10 km) can be performed. However, the increased resolution places a much larger demand on computing resources so such high-resolution forecast runs are typically limited to very regional domains (say, like that over Horry County).

These forecast models can be used in conjunction with available observations to help obtain atmospheric data information where it is lacking. In this process, statistical tools and interpolation techniques are used to assimilate the available observations into the model grid set-up. Missing atmospheric variables and regions from the observations are then provided by the model based on the physical processes governing the model's equations. The end product, called "analysis", is our best-guess atmospheric state that contains real observations and the model's best estimates, based on our understanding of the physical process [*Kalnay et al.*, 1996]. As more observations are available the analysis is performed and verified again to ensure accuracy. As such, the analyses products are very useful in our study of the atmosphere since they provide a global picture of the atmosphere. In fact, the NCEP/NCAR re-analyses and the NASA GEOS-5 analyses (used to make the illustrations in this paper) are essentially produced in the manner described here. In the former data set, the analyses are re-analyzed at NCEP as more observations are available for assimilation. The later data set uses NASA high-resolution model (~15 km spatial resolution) that extends beyond the stratosphere to generate the analyses. These products are well tested with other observations not included in the assimilation process. For weather predictions, these analyses serve as the initial atmosphere state from which the models can predict the evolution of the atmosphere. They also provide the boundary conditions to constrain the model domain. Obviously, the more observations that are used in the assimilation process the better the analyses products, resulting in improved forecasts.

To understand the longer term atmospheric evolution (over a month to an entire season or even decades), atmospheric climate models are used to ascertain the general behavior or tendencies of the atmosphere that we have discussed pertaining the NAM and SSWs. By incorporating the entire stratosphere, these models can extend well above 80 km. For example, the much respected atmospheric climate model called the Whole Atmosphere Community Climate Model (WACCM) developed at NCAR covers the atmosphere from the ground up to about 150 km. As such, to limit the number of grid points (see Figure 11) and remain with the available computing resources, climate models are much coarser than weather models with spatial resolutions of 20-100 km. Furthermore, these atmospheric climate models can be coupled to the oceanic climate models that comprise the Climate System Models. To assess long-term climate states and future climate changes, they will be generally run for months to hundreds of years to predict global changes like the warming trend shown in Figure 1. The ability of the Climate System Models to mimic reality is dependent on the climate observation used to constrain and provide information to the models as they make future prognoses. To date, atmospheric climate models (and climate system models) are very capable of generating realistic NAM patterns. This is not surprising since the NAM is a resonance response of the atmosphere to various atmospheric disturbances.

In summary, analyses products generated by the combination of observations and numerical models (like NCEP/NCAR re-analyses and NASA GEOS-5 analyses) can provide us with arguably the best data set that allow us to study the NAM and SSWs. However, these data products are only as good as the model's ability to mimic observations closely. While these products help us diagnose various mechanisms that may be involved in the variability of the circumpolar flow, they do not give us predictions of what is to come. Only by using these products to initialize the numerical models can we have a prognosis of future atmospheric evolution.

VIII. Sweating the Small Stuff: Gravity Waves

The possible importance of the polar vortex breakdown on the tropospheric weather is shown in Figure 10 and other studies [e.g. *Hurrell et al.*, 2003]. If we can reliably simulate the stratosphere using numerical models with realistic troposphere and stratosphere, then we can improve our prediction skills on the mid-range timescale (a few

weeks to few months). This is because a nearly 30-day time lag exists between SSW onset and the peaking of NAM. Knowing the possible future phase of the NAM will then provide us with addition information to make better weather forecasts and climate assessments. As mentioned above, since the NAM is readily generated in atmospheric climate models, the mid-range forecast should be straightforward.

However, a climate forecast of the stratospheric-troposphere connection proves to be difficult. At present, the better atmospheric climate models like the WACCM fail to simulate SSWs with the right occurrence frequency [*Richter et al.*, 2010]. In a given 50-year run, WACCM generates significantly fewer SSWs than in observations of about 6 SSW events in a 10-year period. Recall that in the NCEP/NCAR re-analyses nearly 25 major SSW events can be identified. This lack of SSW occurrences is puzzling since the climatology of planetary wave and synoptic-scale disturbances in present atmospheric climate models are generally realistic [*Charlton et al.*, 2007].

The reason for this problem may be linked to a type of atmospheric waves that we have neglected to mention thus far. They are called *gravity waves*. Generated by the competing effects of the Earth's gravitational pull and air buoyancy, gravity waves are prevalent in the atmosphere during the wintertime. Of horizontal spatial scale less than 1,500 km and vertical scale less than 30 km, these waves are generated by various mechanisms. The flow of the Jet Stream over large topographical variations like the Rockies and Greenland can promote gravity wave activity that appears to be stationary in time. As shown in Figure 12AB, approaching flow (thick arrow) toward a mountain profile (black shape at the height zero) excites strong alternating bands of vertical motions ("up" and "down" band) indicative of gravity waves. These vertical motions cause ripples in the atmospheric surfaces (line contours in Figure 12B) that are analogous to ocean waves [*Xue et al.*, 2003]. With adequate moisture in the atmosphere, these gravity waves near the mountainous regions appear as bands of clouds as shown in Figure 12C (near the Appalachian mountain range). Adjustment of the atmosphere during the synoptic-scale disturbances can also lead to spontaneous generation of gravity waves near the location of the fronts. These gravity waves eventually drift away from the storm regions. Finally, localized heating in the atmosphere (leading to convection) can readily cause plumes of gravity waves to appear [*Nappo*, 2002].

Once generated, gravity waves can readily propagate through the stratosphere and above [*Fritts and Alexander*, 2003]. While small in the troposphere, gravity wave amplitudes can grow significantly as they encounter thinner stratospheric air and above. As gravity wave amplitudes become very large at varying levels, the gravity wave motion can cause large vertical fluctuation and the atmospheric layer can topple over the layers below leading to "wave breaking" [*Afanasyva and Peltier*, 2001]. As shown in Figure 12D, the breaking process causes vertical swirling of the atmosphere in a manner similar to breaking ocean waves. After wave breaking ends, energy is exchanged between the waves and the circumpolar flow that supports the wave motion. The flow can be accelerated or decelerated as result of this exchange. Damping of gravity wave amplitudes by friction in the stratosphere and mesosphere can also lead to changes in the flow speed. This role of the gravity breaking process and damping is extremely important in the mesosphere and helps maintain the upper portion of the Polar Vortex at its climatological conditions [*Andrews et al.*, 1987].

With oscillatory periods as short as several minutes and spatial scales on the order of 10-1,500 km, gravity waves are generally difficult to observe. This difficulty is exacerbated by the wave's intermittent nature due to variations in generating sources and flow conditions. Given their limited field-of-view, satellite instruments can only infer portions of the total GW variances [e.g. *Wu*, 2004]. Local measurements likewise fail to capture the complete wave structure as gravity waves packets can propagate upward at different rates [*Alexander*, 1998]. As such, gravity waves are not well resolved in the analyses. In addition to lack of observation of gravity waves, the models used to generate these analyses do not have spatial resolution high enough to capture their entire presence.

Figure 13A shows some disturbances related possibly to gravity waves in the GEOS-5 analyses. Here, the gravity waves are suggested by plotting the vertical wind velocity to capture the "up" and "down" motion as noted in Figure

12. Under typical conditions, the atmosphere has very little upward and downward motion (with vertical wind on the average of 1 mm/s) away from strong convection or storm updraft. As such, presence of localized alternating bands of vertical wind (e.g. clusters of adjacent red and blue) strongly suggest the presence of gravity waves. Since the GEOS-5 GCM provides data at every 0.6° longitude and 0.5° latitude, the GEOS analyses holds information on horizontal grid points roughly about 50 km apart across the globe. This coarse resolution causes gravity waves to be blurred and their influence on the flow diminished. We note that the illustration in Figure 13 (10 January 2009) precedes the occurrence of the 2009 SSW.

In using a numerical model with much higher spatial resolution, we can better resolve gravity waves and the importance of their influence on the circumpolar flow. Figure 13B shows the nearly identical atmosphere conditions resolved by a very high spatial resolution numerical model, developed by the author from the ARPS regional weather models to include the entire stratosphere and over the entire polar cap [*Limpasuvan et al.*, 2007]. Providing information on horizontal grid points at 10 km apart on the entire globe, this model is roughly 5 times as "sharp" as the GEOS-5 and offers a "high-definition" (HD) view the atmosphere and gravity waves. As illustrated, the features hinted in the GEOS data are much better defined. For example, we see a clearer picture of gravity waves generated over the Scandinavian terrain and the Western Canadian Cascades that grow in altitude as the waves propagate in the upper stratosphere.

The effects of spatial resolution are illustrated in Figure 14. Suppose we have a spatially repeating disturbance (magenta curve in Figure 14A) that we are trying to understand by observations. We initially attempt to measure it by placing the blue sensors at an equidistance of 10 km apart. At that distance, based on our observations, we may interpret that the present disturbance repeats itself every 40 km (as shown in Figure 14B) and has a very large scale compared to the actual disturbance. However, if we buy more sensors (red) and place them at an equidistance of 5 km between the blue and red sensors (Figure 14A), our new observational network has now doubled in spatial resolution. You can then infer that the observed disturbance from this new network of sensors will reveal that the disturbance has much more structure and is more akin to the real signal. As illustrated also in Figure 13, the problem here is clearly the resolution which we use the study the disturbance. In the atmosphere, phenomena like gravity waves can occur at scales smaller than our global data and models can resolve. Unfortunately, these waves prove to be a very important component of the atmosphere.

IX. Dealing with Waves

Unlike trading in your old television set for a new HD television, the benefit of high-resolution models in better resolving these gravity waves is more than aesthetics. Like planetary waves and synoptic-scale disturbances, gravity waves are essential components of atmospheric disturbances (Figure 15). Along with planetary waves, gravity waves are dominant in the stratosphere and mesosphere. The exchange of energy between these waves and the circumpolar flows at these lofty heights are crucial in maintaining the overall structure of the atmosphere that dictates our climate. In particular, the wave-flow interaction helps drive a slow overturning pole-to-pole motion (shown as yellow arrows) that produces slow sinking of air into the winter Polar Vortex and rising motion in the summer pole. The roles of gravity waves are particularly very important in the upper mesosphere where breaking of gravity waves is prevalent. The breaking process greatly decelerates the circumpolar flow in the upper mesosphere and causes the circumpolar winds to diminish with height. As shown in Figure 9, these waves are also essential in the circumpolar wind variability we observe in the atmosphere such as the case of SSWs.

In the absence of these wave disturbances, the atmosphere would be significantly different from observations. Figure 16 shows the effects of these waves on the atmospheric temperature distribution. With these waves, the various chemical constitutions (like ozone, carbon dioxide, and water vapor) interact with the incoming solar energy and the outgoing energy emitted from the Earth's surface to differentially heat the various parts of the atmosphere.

As computed by *Fels* [1985], the resulting temperature field excluding waves would reveal that the coldest region in the atmosphere appears in the winter pole in the Northern Hemisphere mesosphere (as marked by the dashed rectangles). This region corresponds to the location where the atmosphere would be completely dark due to the tilt of the Earth's axis away from the sun during the wintertime. However, with the presence of atmospheric wave disturbances, the observed temperature field is quite different. The observed coldest region is actually in the polar *summer* mesosphere, and the polar winter stratosphere and mesosphere are considerably quite warmer (see dashed rectangles). The reason for this unexpected structure is slow overturning pole-to-pole motion (shown as yellow arrows in Figure 15) that produces slow sinking of air into the winter Polar Vortex and rising motion in the summer pole. This motion is driven by the interactions of waves and the circumpolar flow above 40 km. The persistent sinking of the air into the winter polar vortex causes air to compress and become warmer than the scenario with no waves. This is analogous to the warming of the bicycle pump piston when you rapidly displace the plunger. On the other hand, the rising motion over the summer polar region causes air to expand and become cooler than the scenario devoid of waves.

With a much coarser computational grid size (spaced grater than 500 km apart) than the GEOS-5 data, climate models cannot explicitly resolve gravity waves. Recall that these models have no issues with planetary waves and synoptic-scale disturbances. However, because gravity waves are extremely important in maintaining the overall climatology of the atmosphere, their effects must be somehow included in the model in order to simulate a reasonable stratospheric and mesospheric evolution. The only reason why the GEOS-5 data can produce SSWs (as shown, for example, in Figures 7 and 8) is because the data product subsumes real observations through its assimilation model.

In practice, the effects of GW are included in atmospheric climate models through mathematical parameterization schemes. The statistics of potential gravity wave sources and locations of wave perturbations (like mountains and regions of strong convection) near the surface and throughout the troposphere are identified using available (albeit *few*) observations. These statistics are correlated with large-scale meteorological features (like winds and temperature) that can be readily resolved in the models. The wave amplitudes are assumed to grow in height (like in the stratosphere and mesosphere) where they can eventually cause an overturn in the atmosphere layers and break (as seen in Figure 12D). The parameterization arbitrarily sets a threshold of the amplitude where breaking may occur and the momentum and thermal influence of the gravity wave dissipations are incorporated into the atmospheric governing equation used in the model [e.g. *Lindzen*, 1981].

Despite the good (and clever/practical) intentions of these parameterization schemes, the wave sources are crudely specified since observing these waves are difficult (as discussed previously) and details of the waves are still in an infant stage. Presently, the specified wave sources are associated with primarily orography and convection. Wave sources due to spontaneous sources like synoptic-scale disturbances are not yet included. To simulate the proper atmospheric climatology, atmospheric climate modelers haphazardly *adjust and tune* the parameterization values to emulate the appropriate gravity wave mean-flow forcing effects [*Andrews et al.*, 1987]. As such, gravity wave parameterization schemes (varying widely in complexity) and how they are tuned remain largely unconstrained [*Fritts and Alexander*, 2003] among differing atmospheric climate models. This degree of freedom in these schemes may contribute to the temperature uncertainties in the IPCC global warming trend shown in Figure 1.

With present parameterization schemes, these climate models have difficulty in generating SSWs of proper occurrence frequencies. While these models can account for the NAM appearance, the lack of realistic stratosphere and mesosphere simulation in these models hinder our prognostic insight on the coupling of the NAM to the atmosphere above 12 km. Recently, by expanding GW parameterization to include the generation of GW by synoptic-scale disturbances, the WACCM model is able to produce simulations in which the occurrence frequency of SSWs is closer to observations [*Richter et al.*, 2010]. While the new parameterization is preliminary and still very crude, the improvement in the model results further emphasize the importance of gravity waves in the variability of the stratosphere and the possible generation of SSWs [*Siskind et al.*, 2007].

X. Summary and Discussion

Despite the complexity of our atmosphere, we can derive at its dominant global pattern embodied by the *Northern Hemisphere Annular Mode* (NAM). As the leading mode of atmospheric climate variability, the NAM describes the fluctuation of the entire atmospheric mass across the Arctic Circle that dictates the behavior of the troposphere and stratosphere. Its appearance is a manifestation of the atmosphere's natural response to random disturbances and accounts for nearly a ***third*** of all changes in the wintertime meteorological conditions (Figure 6). In the positive phase of the NAM fluctuation, the cold atmospheric mass is anomalously equatorward (with respect to the climatological state). The Jet Stream and associated synoptic-scale storm activities are displaced equatorward. The stratospheric Polar Vortex tends to be warmer with weaker circumpolar flow. In its negative phase, cold atmospheric mass is confined inside the Arctic Circle. Synoptic-scale storm activities are shifted closer to the North Pole and the Polar Vortex is unusually strong. These NAM phases alternate in time on a wide range of timescales (daily, monthly, and yearly) with varying strength of anomalous metrological conditions.

In drawing analogy of NAM to something that we are all familiar with (i.e. our own body), we can think of the fluctuation in the NAM pattern between its high and low phase as being analogous to our beating heart. Indeed, in accounting for the majority of the atmospheric behavior, the NAM is the very much the "heart" of our atmosphere that beats in time and contracts/expands as the atmospheric mass fluctuates across the Arctic Circle. From this point of view, the atmosphere is a "living and breathing" entity that forms a *symbiotic* relationship with all it envelops: humans, animals, rocks, and ocean. The alternating phases of the NAM's pattern reflect the changes in our weather patterns and the overall tendencies of our atmosphere in a way that suggests how the various parts of our bodies (e.g. lungs and chest cavity) fluctuate in concert with our own heart. The beating of the NAM "heart" (as seen in its index) is irregular and non-predictable since the NAM is a natural response to random disturbances. The NAM presence occurs independently from external forces such as increasing carbon dioxide, changing solar radiation, and emissions from volcanic activities. However, the beating trend of the NAM can be influenced by these external influences [*Hurrell et al.*, 2003]. Hence, to fully assess future atmospheric climate changes, we must understand the NAM.

While the NAM is still relatively unknown to the general public, another (and more popular) example of a large-scale pattern of climate variability is the El Niño/Southern Oscillation (ENSO). The existence of ENSO is due to coupled ocean/atmosphere interactions in the tropical Pacific region and explains the largest variance of the large scale climate variability pattern in the tropics. On the other hand, the NAM owes its existence to internal atmospheric dynamics in the middle to high latitudes. As such, it is the most important pattern of climate variability in the Northern Hemisphere [*Thompson and Wallace*, 2001]. We note that anomalous changes in the sea surface temperatures related to ENSO can also contribute to changes in the atmosphere at high latitudes [e.g. *Limpasuvan et al.*, 2005].

The internal atmospheric dynamics in the middle latitudes are dominated by wintertime wave disturbances of different spatial (and temporal) scales (Figure 15). Planetary waves are of continental scale and their energy continually propagates from the troposphere into the upper stratosphere where they can disturb the Polar Vortex. Of scale smaller than 1,500 km, gravity waves are ubiquitous in the troposphere as strong winds flow over topography and the atmosphere undergoes thermal and momentum adjustments. They can also readily propagate into the stratosphere and the mesosphere where they help maintain the atmospheric structure at those high-altitude regions. With spatial scale between planetary waves and gravity waves, synoptic-scale wave disturbances are active as extra-tropical storms travel the globe affecting our daily weather patterns. Energies associated with these synoptic-scale waves are largely confined in the troposphere. Overall, all these atmospheric waves play a key role in distributing momentum and heat in a similar manner that waves and ocean currents (like the Gulf Stream) do in the prevailing ocean circulation. In the absence of these waves, the atmosphere will be much different from what we observe (Figure 16).

Occasionally, anomalously strong planetary wave activity penetrates into the polar stratosphere (Figure 9). The interaction of planetary waves and the polar stratospheric flow leads to tremendous warming of the frigid and dark Polar Vortex – a phenomenon referred to as *sudden stratospheric warming* (SSW). During this interaction, the flow around the vortex becomes highly distorted as the Polar Vortex is displaced very far from the North Pole or is broken into smaller vortices (Figure 8). During SSWs, the circumpolar flow (averaged around the latitude ring) greatly weakens and can eventually reverse in direction (Figure 7). The triggering of SSW is still an open research question. Gravity waves are ubiquitous in the stratosphere and can interact strongly with the Polar Vortex [*Limpasuvan et al.*, 2007]. Their roles in SSWs are still under investigation.

The "heart" of our atmosphere is sensitive to the unusual occurrence in the stratosphere and mesosphere. In particular, the weakening of the Polar Vortex during the SSW onset induces the NAM toward its negative phase. At least a 30-day lag exists between the incipient SSW stage (when the atmosphere is near its climatological state) to when the NAM becomes fully realized in its negative phase (Figure 10), corresponding to wintertime conditions in which the Jet Stream retreats closer to the Arctic Circle. Such lag suggests that variability in the stratospheric Polar Vortex yields a useful lev*el of predictive skill for Northern Hemisphere wintertime forecast on both intraseasonal and seasonal timescales [Hurrell et al.*, 2003]. That is, if we observe changes in the Polar Vortex leading potentially to SSW, then we can improve how we make future weather and climate forecasts near the surface, based on the expected change in the NAM index to follow. To continue our analogy, the 30-day lag suggests that the drastic event in the circulation breakdown in the stratosphere and mesosphere (i.e. SSW) can provide a sharp "jolt" to the beating NAM, making it arrhythmic with respect to its natural fluctuation. As such, to complete our understanding of atmospheric climate variability, the role of the stratosphere and mesosphere is obviously very important. It is important to note that, like the NAM, polar warming related to SSW is a naturally occurring phenomenon.

Historically, atmospheric physicists focus mainly on the troposphere, and the stratosphere and the mesosphere are called collectively the "ignorosphere". In addition to fact that our lives come in direct contact with the troposphere (i.e. weather), the main reason for such bias toward the troposphere is the fact that it accounts for ~80% of the total atmospheric mass. The troposphere air is much denser than the stratosphere. We know this from experience when we travel to places of high altitude (like Denver, Colorado) where breathing can become difficult. The implication that the much thinner stratosphere (related to SSW events) can influence the much denser (and more massive) troposphere (as embodied in the NAM) seems initially very farfetched. However, recent studies are revealing that the changes in the circumpolar flows during SSWs alter the propagation of various atmospheric waves originating below from troposphere. This altered wave influence in turn changes the circumpolar flow at subsequently lower and lower levels below the stratosphere. The wave influence eventually helps to redistribute atmospheric masses into the configuration of low NAM phase [*Baldwin and Dunkerton*, 2001; *Limpasuvan et al.*, 2004]. In other words, the wispy stratospheric changes can influence the hefty troposphere by turning the tropospheric energy against itself.

Current atmospheric climate models are important components of the climate system models used to help us assess changes in the climate system and make predictions (Figure 1). While current atmospheric climate models can readily generate the NAM, these models have difficulty simulating the proper rate of occurrence of the observed SSWs and the proper climatology of the stratosphere and mesosphere. Therefore, these models fail to properly capture the all of the natural changes in the NAM due to the ignorosphere. This shortcoming is rooted to the lack of spatial resolution of these models (Figures 13 and 14). With poor resolution, an important class of atmospheric waves is missing entirely: gravity waves. These waves are crucial in maintaining the climatological state and variability of the stratosphere and mesosphere. Instead, the effects of gravity waves are emulated through mathematical schemes. Scientists running atmospheric climate models can haphazardly tune these schemes into order to mimic the observed atmospheric conditions. The tuning parameters are largely unconstrained since observations of gravity waves are difficult [*Fritts and Alexander*, 2003] and may contribute to the uncertainties in present climate system models (Figure 1).

Obviously, issues with poor spatial resolution can be improved by increasing the number of grid points in the model domain (Figure 11) so that spacing between adjacent grid points is closer (10 km or less). However, given the current computing technology, ramping up the spatial resolution of atmospheric climate models is not practical for running global simulations over a month, a year, or a few decades, especially when these models are extended higher in altitude to include the mesosphere. While such long-term, high-resolution climate runs will better address the connection of NAM and the stratosphere/mesosphere evolution, data output would be very large. The simulation will also take a very long time to complete due to numerical instability issues which require that increasing spatial resolution must be accompanied by decreasing the model integration time steps.

Regardless, scientists are starting to experiment with simulating the atmosphere at extremely high spatial resolution [e.g. *Hamilton et al.*, 2008]. Technical issues are met and slowly overcome. As computing and engineering technology continues to advance, increasingly high-resolution climate models will become more practical and should contribute greatly to our understanding of the atmosphere [*Hamilton*, 2008]. As seen in Figure 13, high-resolution models (like ARPS) can readily reveal gravity waves in the stratosphere and, more importantly, their effects on the circumpolar flow. In fact, future efforts of climate system models at NCAR (as highlighted at the University Center for Atmospheric Research [UCAR] Annual Meeting 2009 attended by the author) are aimed at merging high-resolution weather models (like ARPS) with present atmospheric climate models to resolve small-scale phenomena like gravity waves and clouds. While the discussion of clouds is beyond the scope of this paper, it is worth noting that the presence of clouds is extremely important in the energy balance of the atmosphere [*Hartmann*, 1994]. Like gravity waves, clouds can appear at very small spatial scales, and their current representation in climate models is accounted for by numerical parameterizations. The efforts at NCAR/UCAR will involve the construction of one of world's fastest supercomputing center (with funding from the National Science Foundation) to run the next generation of high-resolution climate models.

To this end, it appears that future generations of scientists will have the tools needed to better understand atmospheric climate variability. With improving computing facilities (allowing for climate models of higher resolution) and potentially better techniques to observe the atmosphere, future scientists can better diagnose the behavior of the NAM (the heart of our atmosphere) and how it fits into the framework of the entire atmosphere. In particular, with future improvement of stratosphere and mesosphere simulations and nearly all atmosphere waves resolved in future models, we can improve our understanding of the connection between NAM and SSW. We can use these high-resolution models to better assess future climate changes with fewer uncertainties – allowing us to make better decisions and evaluate our influence on the environment. At present, our ability to diagnose the beating "heart" of the atmosphere is incomplete.

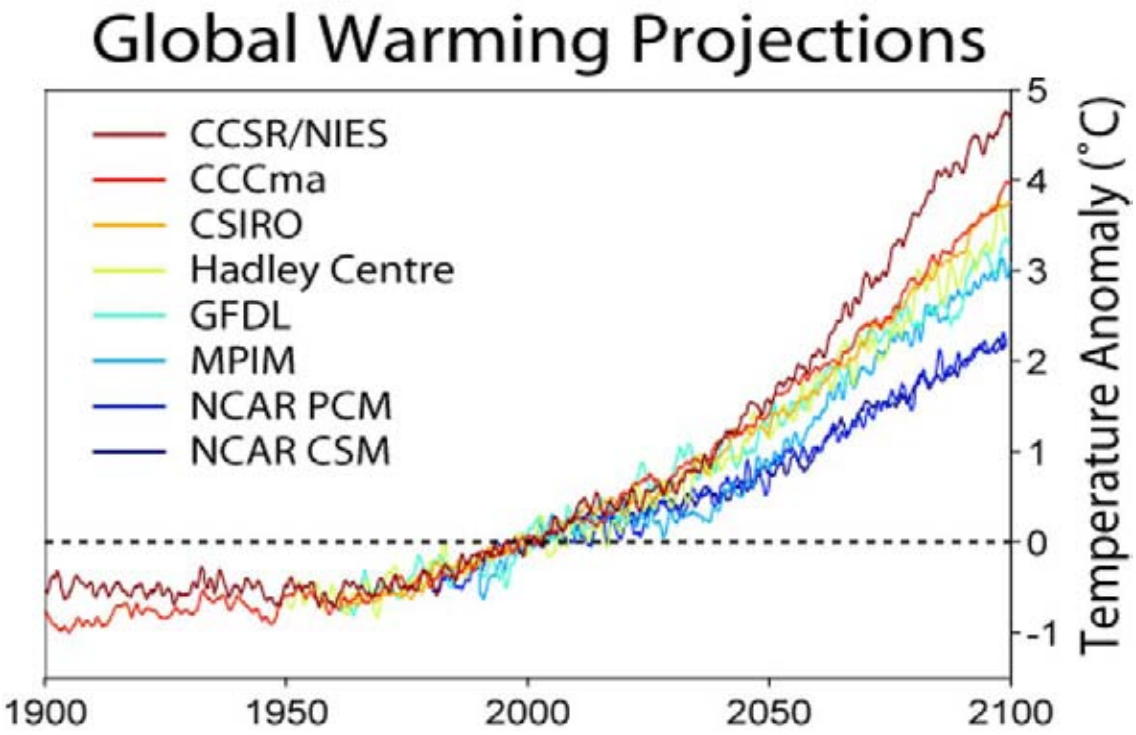

Figure 1

The projection of global temperature change relative to the year 2000 based on various numerical climate system models. The figure is from the IPCC Third Assessment Report [2001].

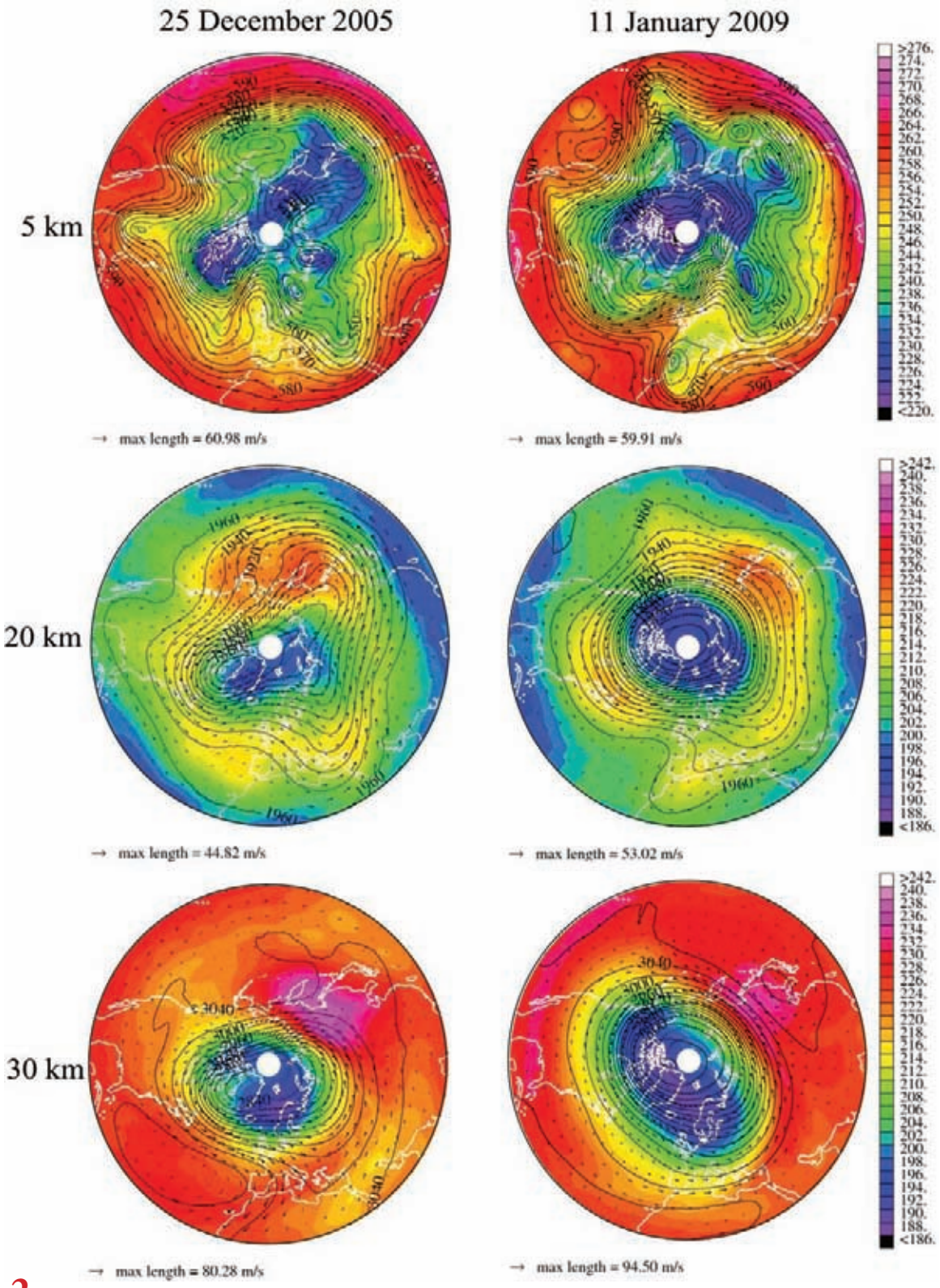

Figure 2

A snap-shot view of the atmospheric flow and temperature on 25 December 2005 (left column) and 11 January 2009 (right column) at the altitude of 5 km (in the troposphere), 20 km (in the lower stratosphere), and 30 km (in the middle stratosphere). The line contours are essentially streamlines that guide the atmospheric winds (arrows). The maximum wind speed at each level is shown with each plot. For reference, 25 m/s is about 51 miles/hour (mph), 50 m/s is about 112 mph, and 100 m/s is about 223 mph. Color maps indicate temperatures in degree Kelvin (K). For reference, 290 K is about 63°F, 273 K is 32°F, and 200 K is roughly -100°F.

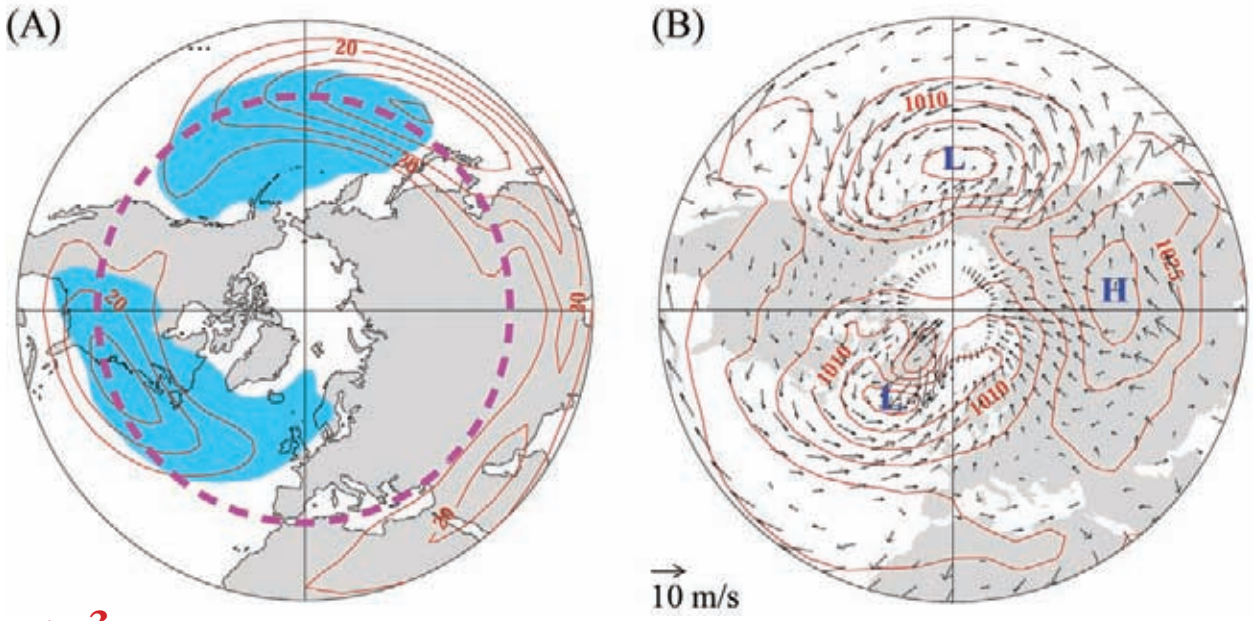

Figure 3

A NCEP/NCAR climatology (1958-2001) of the wintertime (December-January-February) of the Jet Stream wind strength at 5 km (A) and the sea level pressure (SLP) at the surface (B). In illustration A, the red contours are given at 5 m/s intervals and indicate wind blowing in the west-to-east direction. The blue areas show the climatological regions of storm activities. The 30°N latitude circle is overlaid as a dashed, magenta circle. In illustration B, the arrows show the surface winds. The reference arrow shows the length of the arrow with wind speed of 10 m/s speed.

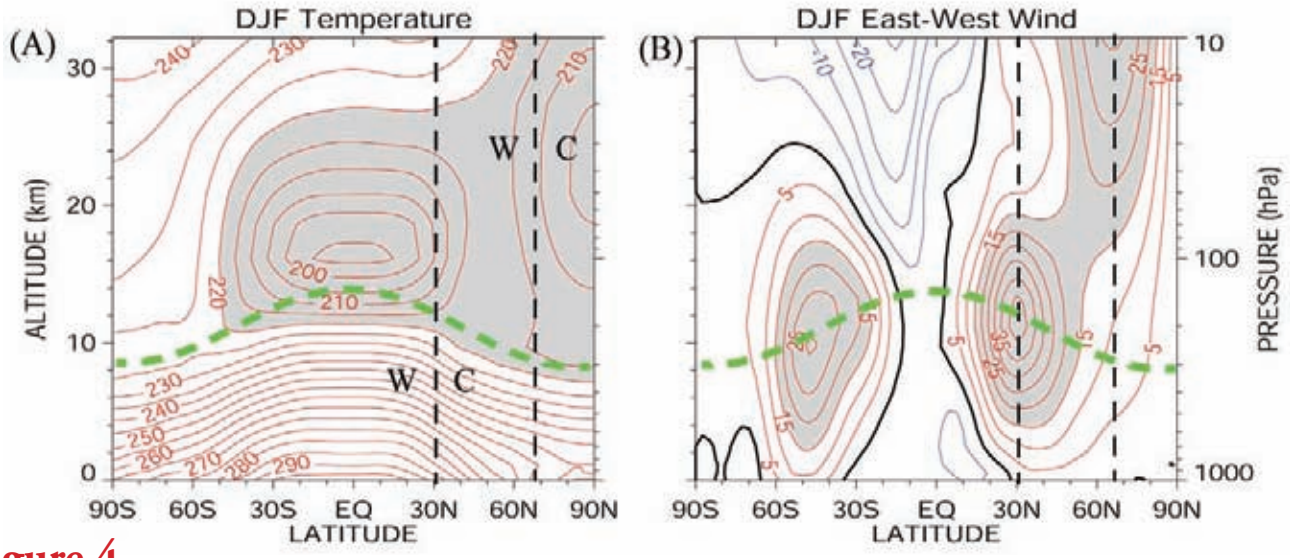

Figure 4

Latitude-altitude cross-section of the temperature and wind averaged along each latitude circle during December, January, and February in the 44-year NCEP data record (1958-2001). In the wind distribution, the contour values are given every 5 m/s; the red contours indicate the west-to-east flow and blue indicate the east-to-west flow. The temperature contour values are given every 5 Kelvin. The vertical dashed lines locate the latitude of the Jet Stream and the Polar Vortex core. The dashed green line marks the tropopause or the boundary between the troposphere and the stratosphere. The gray shadings highlight regions of cold air and strong winds.

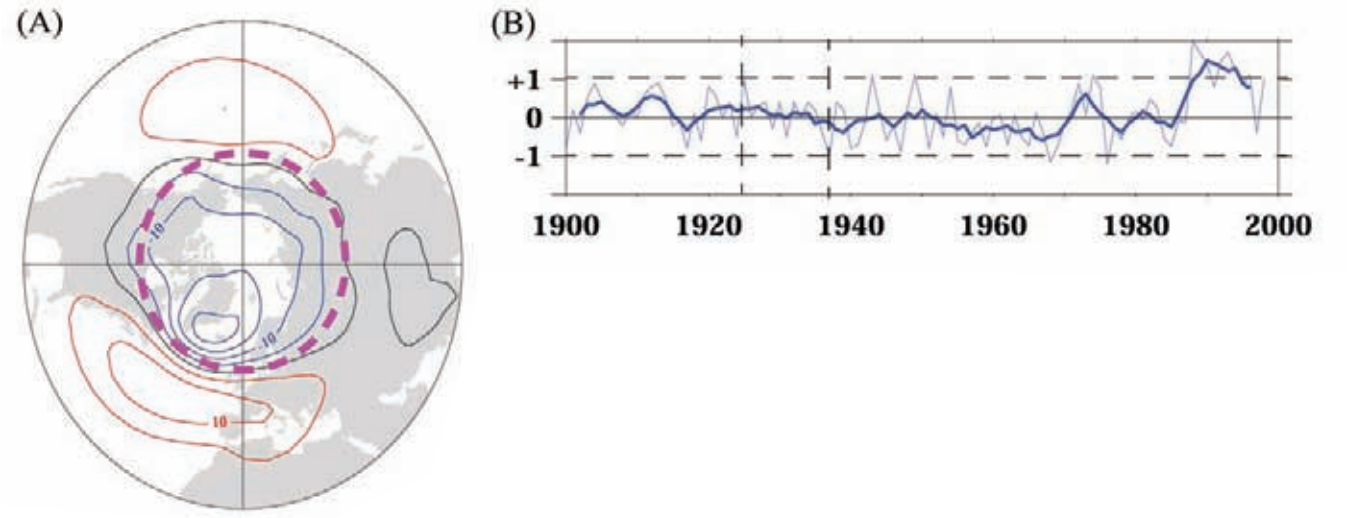

Figure 5

The Northern Hemisphere Annular Mode (NAM). (A) The see-saw pattern of the sea level pressure anomalies (departures from climatology) as described by the NAM when its index is positive and of unit value. Blue (red) contour is lesser (greater) than climatology. (B) The NAM time series (NAM index).

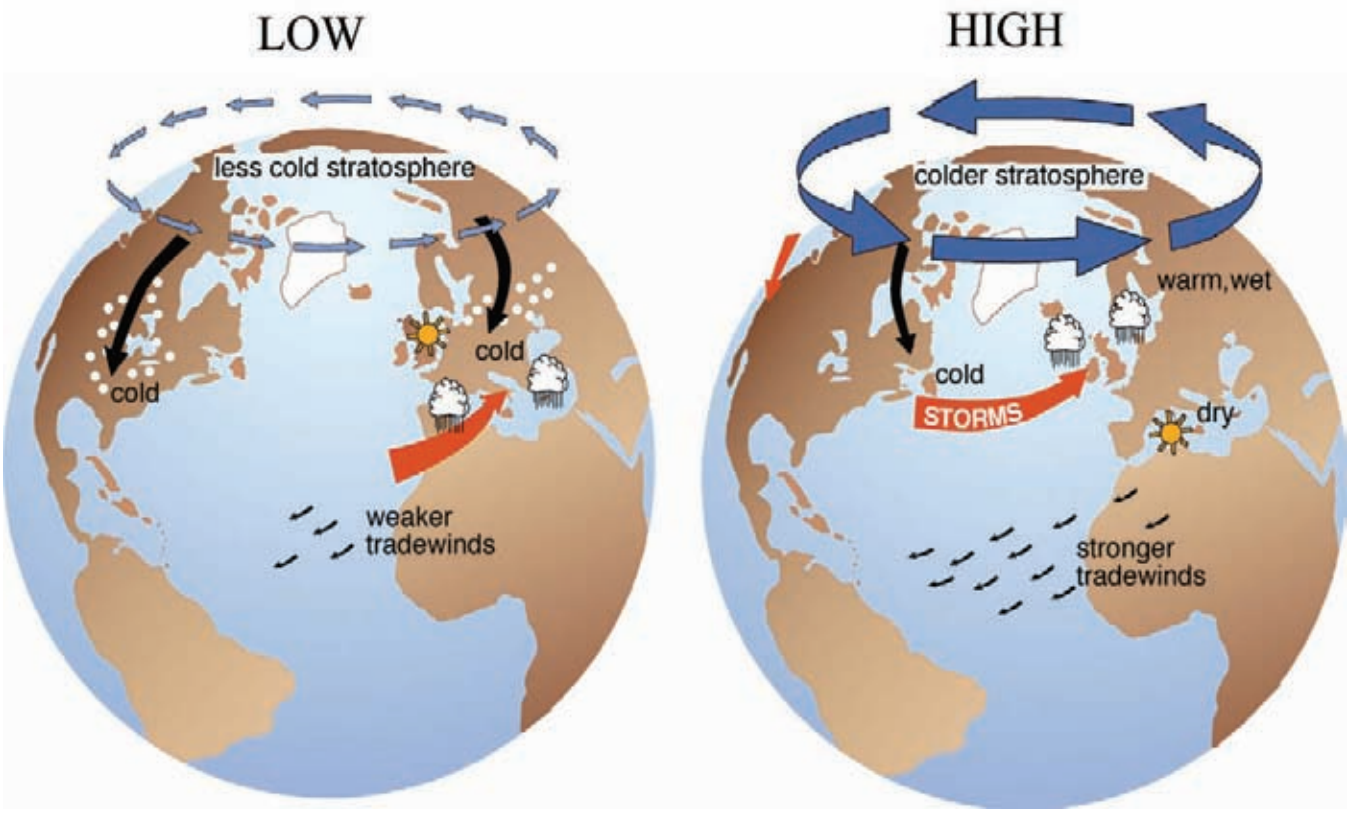

Figure 6

Various near-surface meteorological conditions associated with the low and high phase of the Northern Hemisphere Annular Mode (NAM). Courtesy of Prof. David W. Thompson (Colorado State University).

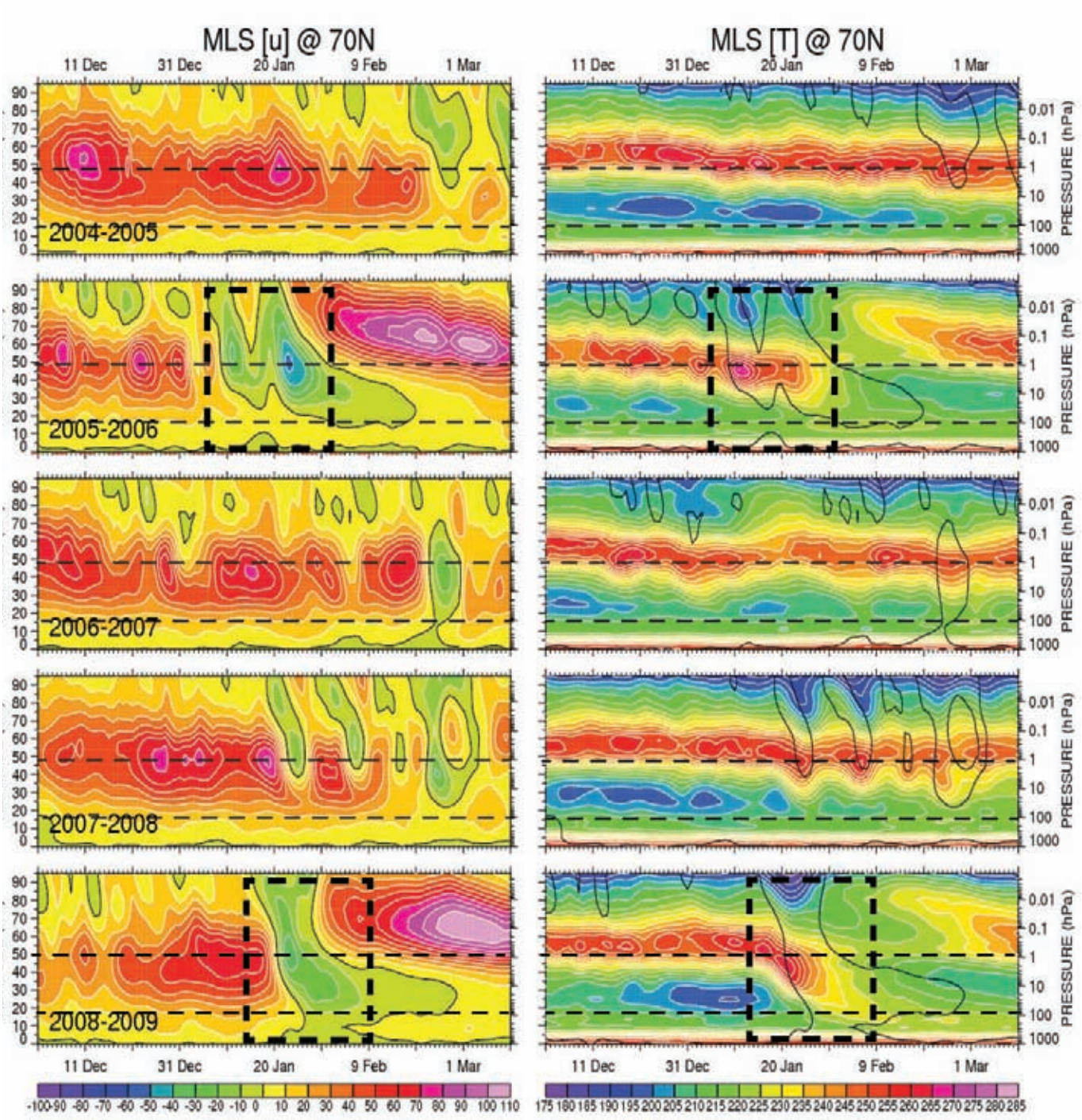

Figure 7

Changes in the circumpolar wind strength/direction (left column) and temperature (right column) averaged at 70°N latitude circle during recent winters. In the left column, wind in the west-to-east direction is shown in the reddish tone with positive values. Wind in the east-to-west direction (reversal in the typical circumpolar wind) is given green-bluish tone and negative values. In the right column, colder temperature is bluish in color and warmer temperature is reddish in color. The black contour denotes the location of the zero wind. Long tick marks in the time axis are shown every ten days. The dashed horizontal line marks the upper boundaries of the troposphere and stratosphere. The dashed box indicates the occurrence of sudden stratospheric warmings (SSWs).

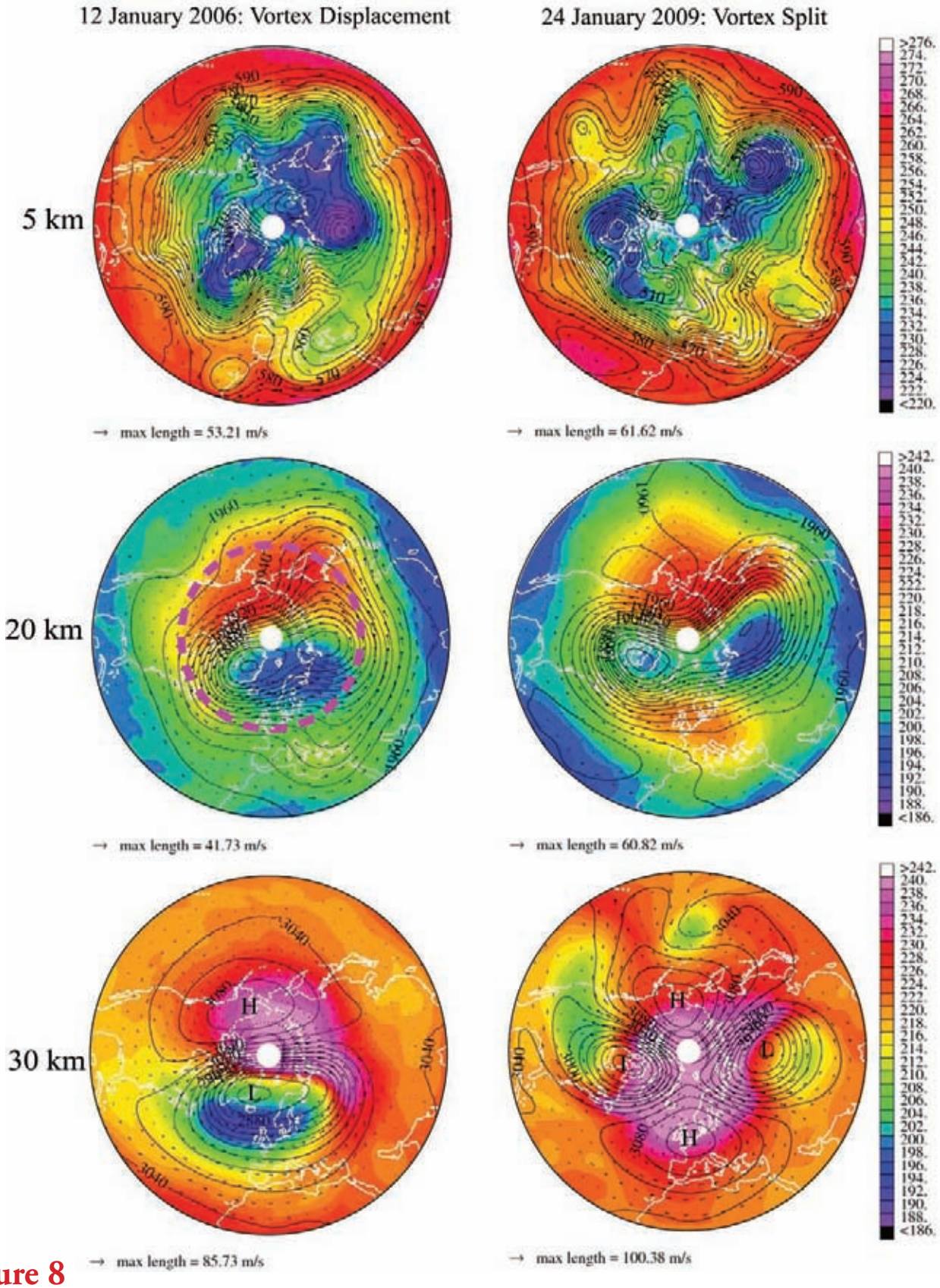

Figure 8

Recent sudden stratospheric warming (SSW) events in January 2006 (left) and 2009 (right). The 2006 SSW event is characterized by a strong vortex displacement off the North Pole. The 2009 SSW event developed as the polar vortex split. The plotting convention is the same as Figure 1.

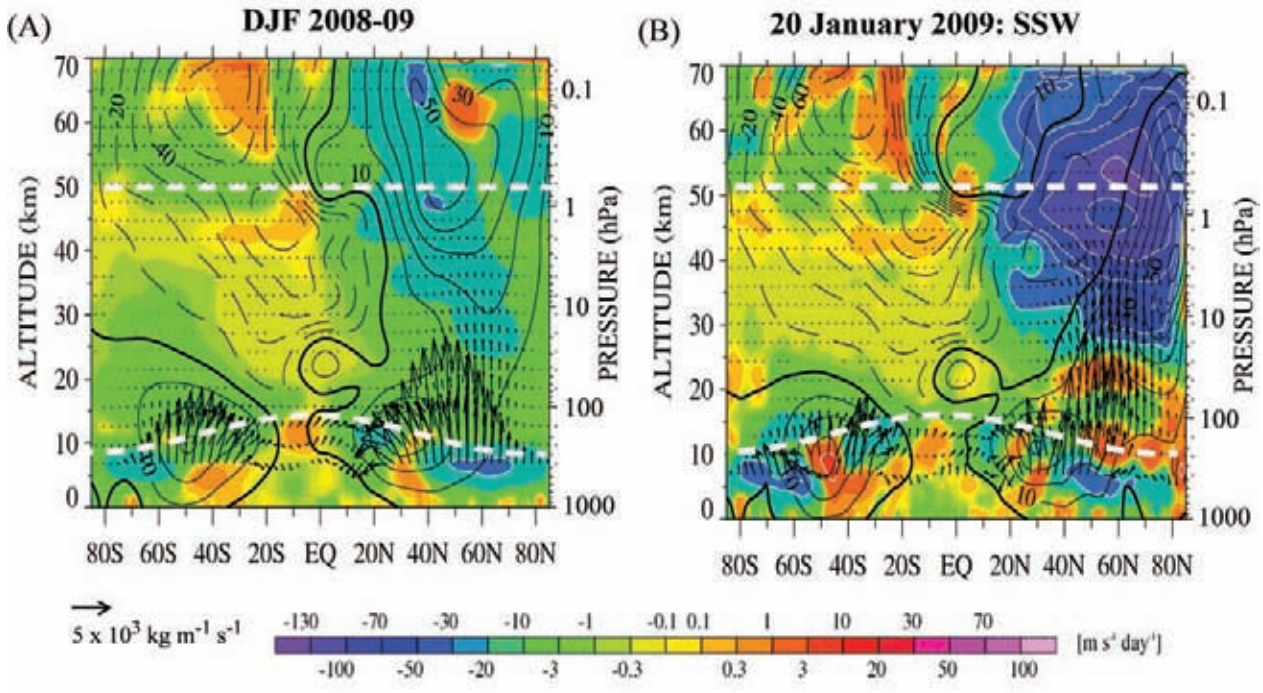

Figure 9

Planetary wave energetics (arrows) and their influence (color-filled contours) on the latitudinally averaged winds. (A) The typical wave propagation and influence during 2008-09 winter. (B) The typical wave propagation and influence during SSW of 2009. Data analyzed from NASA GEOS-5 analyses.

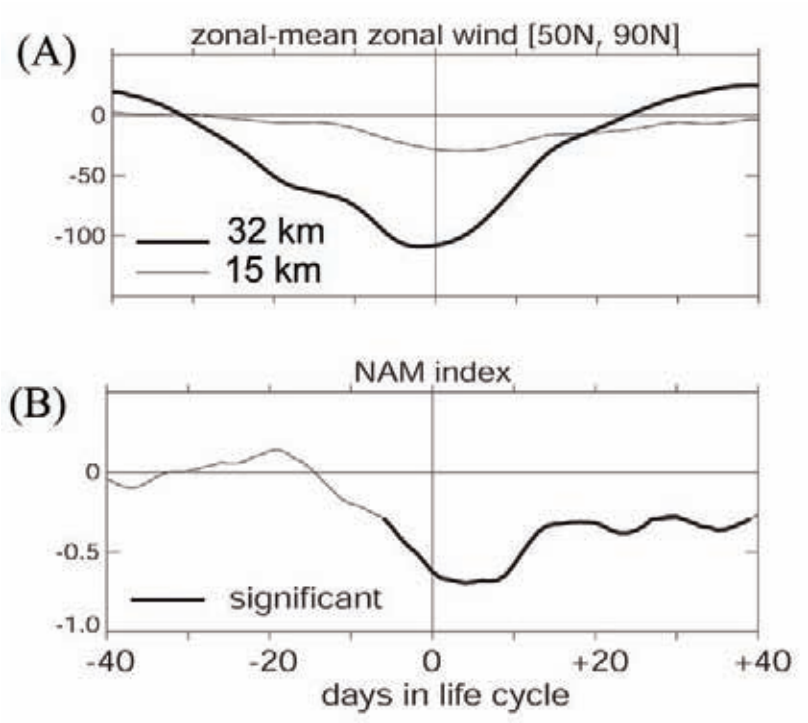

Figure 10

Composite structure of the Polar Vortex winds (A) and NAM (B) with respect to the SSW life cycle. The central date of the life cycle (i.e. day "0") corresponds to when the SSW episode is fully matured (i.e. when the polar wind is moving east-to-west at the greatest speed at 15 km). Positive days mark the recovery of SSW after maturation. Negative days mark the onset and growth of SSW prior to maturation.

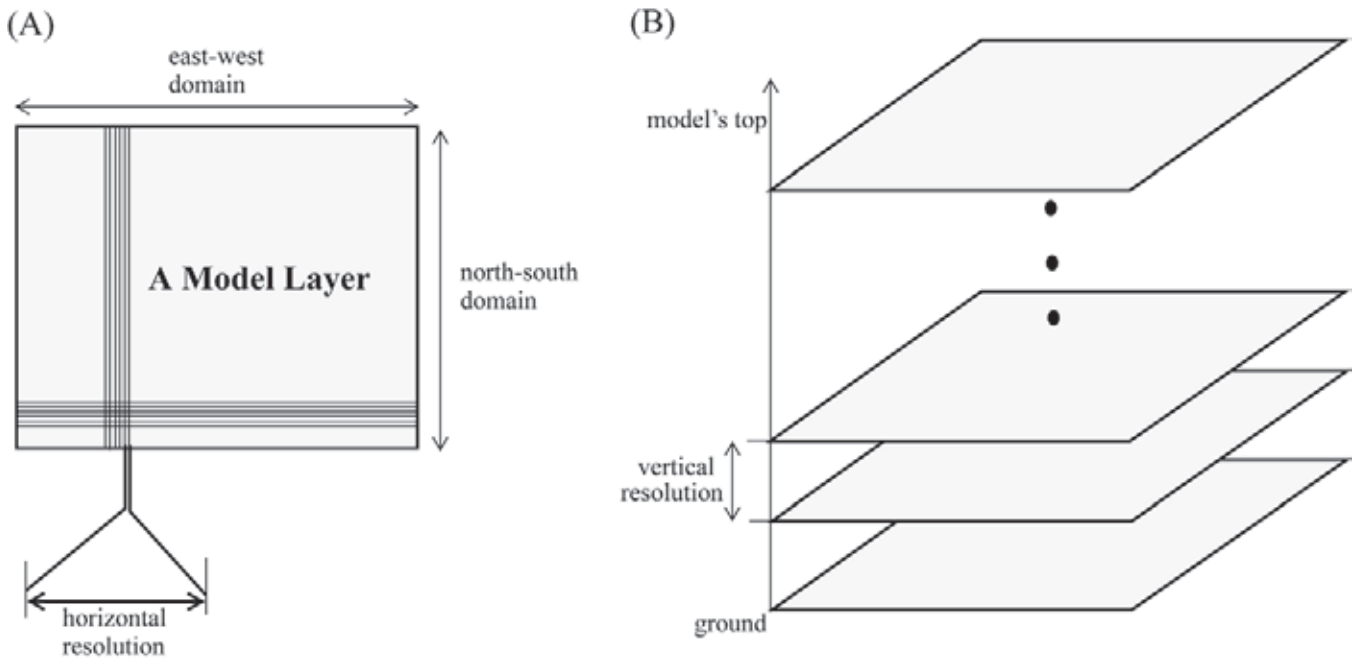

Figure 11

Typical set-up of a computer model used to predict the atmosphere. (A) At a given layer, the atmospheric domain is divided on the many grid points (shown as dots). The spacing between the dots determines the model horizontal resolution. (B) The entire atmosphere is made up by stacking these model layers from the ground up to the predetermined height of the model's top.

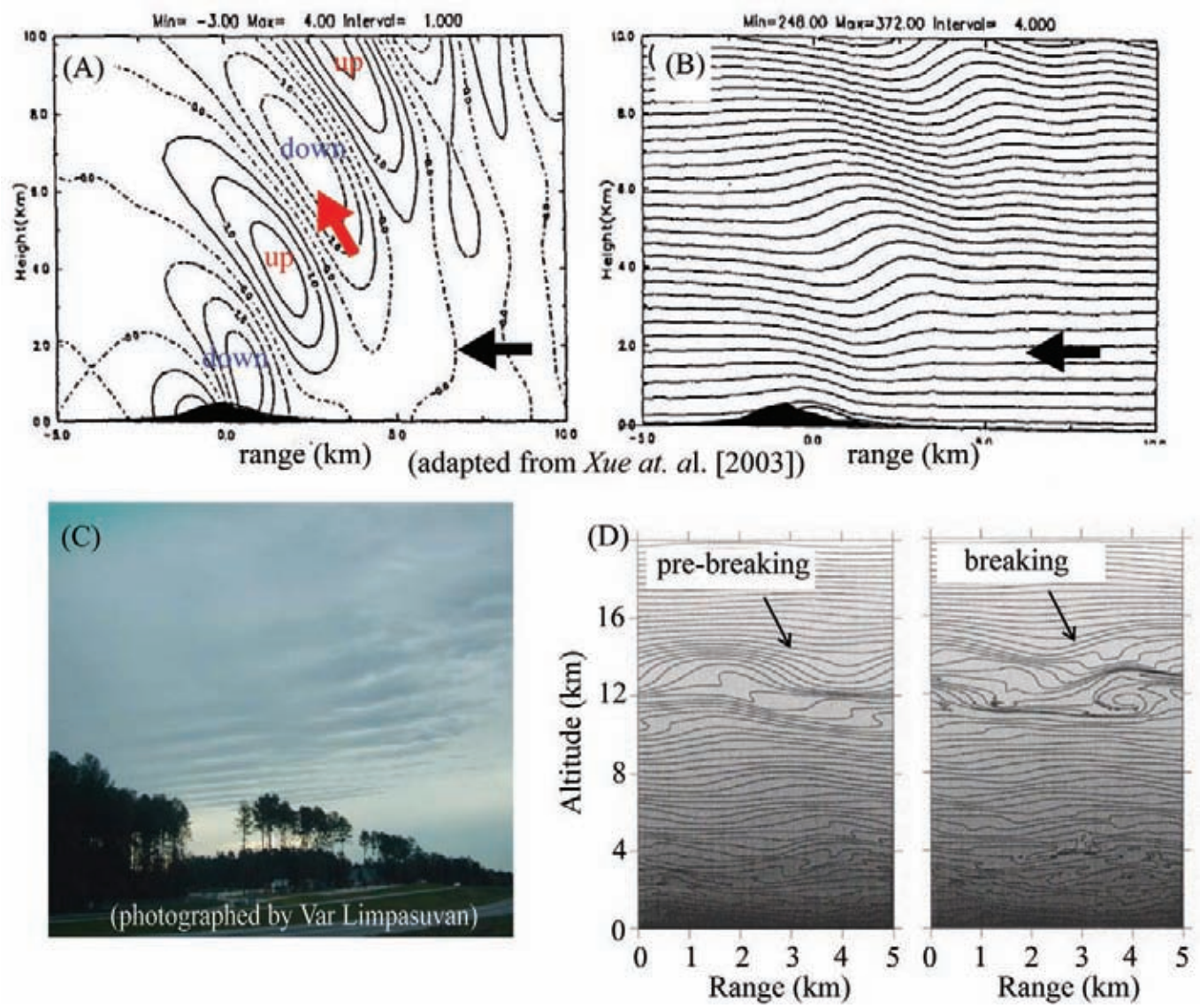

Figure 12

The gravity wave generation and its breaking. (A) A model's formation of gravity waves as strong wind (thick black arrow) approaches an idealized mountain (black filled shape at ground level). Upward and downward motions are shown as solid and dash contours, respectively. The red arrow indicates the direction of wave energy propagation. (B) Same as (A) except for the "streamlines" separating the vertically stacked air layer. The perturbation in the streamlines is related to the up and down motion of the wave. (C) Gravity waves can be seen in the Carolina downstream of the Appalachian Mountain range. This was taken on a drive toward Asheville, NC. (D) A model simulation of gravity wave breaking by *Afanasyva and Peltier* [2001]. Note the likeness to breaking of oceanic waves and the swirling vertically-stacked fluid layer.

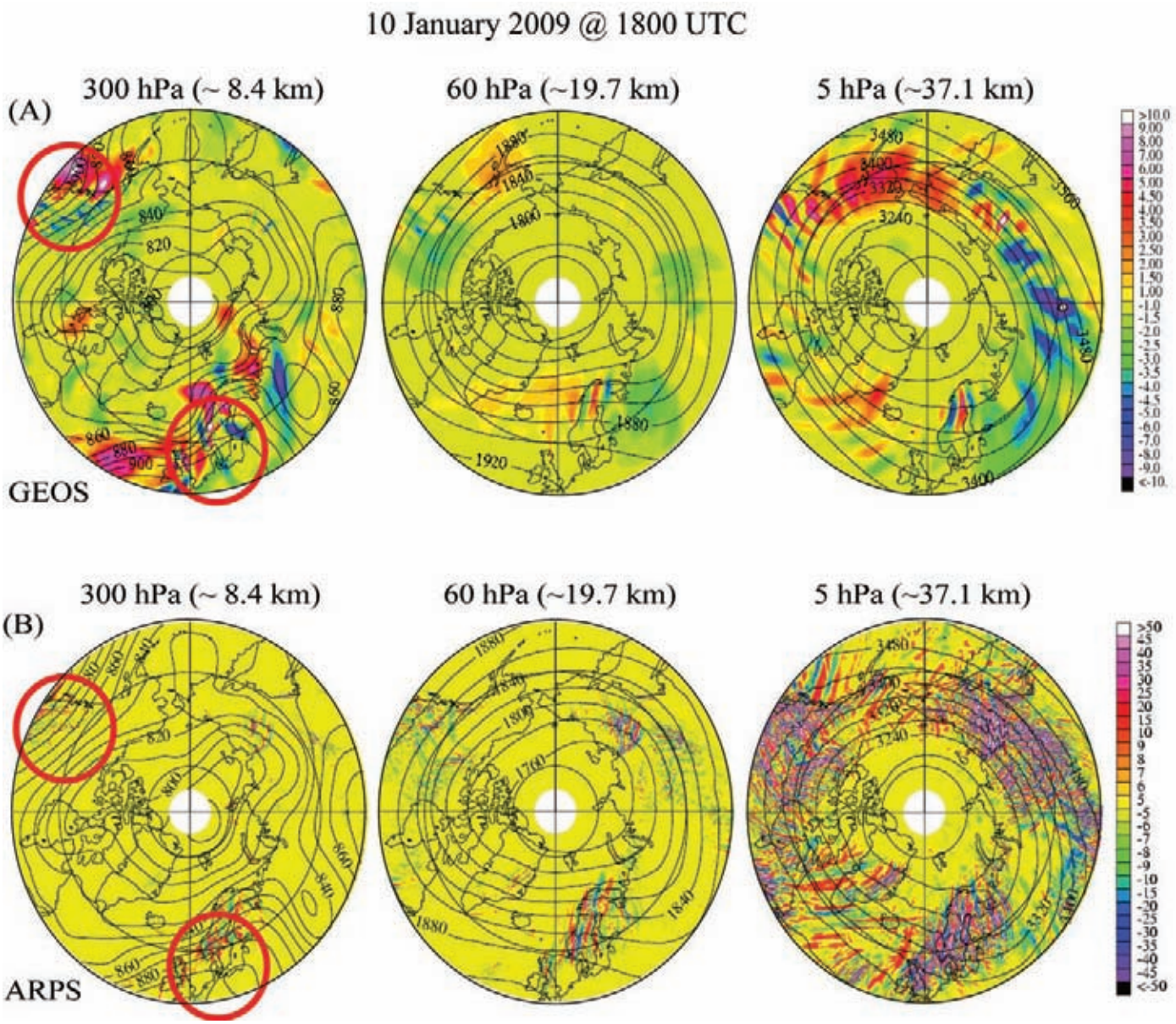

Figure 13

The circumpolar flow on 10 January 2009 as generated by the GEOS analyses (A) and the ARPS model (B). Streamlines are shown as contours (and wind arrows are omitted for clarity). The superimposed colors show the presence of gravity waves. Note that since the waves in the GEOS analyses are weaker than those found in ARPS the color contour values are different. Each column shows the atmospheric structure at different altitude levels as marked. The red circles are regions of gravity waves discussed in the text.

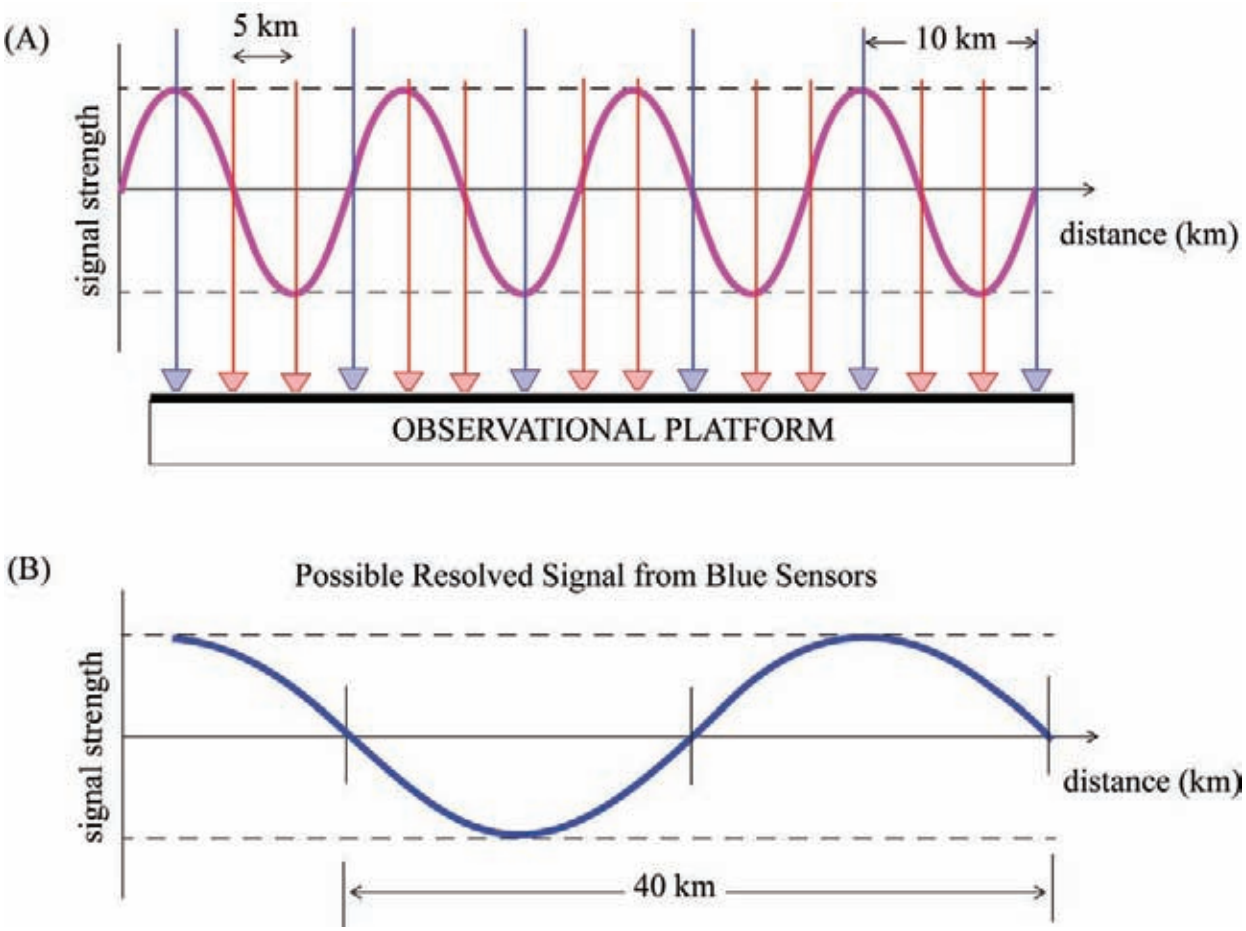

Figure 14

The effects of spatial resolution. (A) An idealized spatially repetitive signal (magenta curve) as a function of distance is being sampled by first the blue sensors (spaced every 10 km apart) then later in combination with the red sensors (spaced every 5 km apart). (B) By hypothesizing that the disturbance is spatially repetitive, a possible interpretation of the signal observed by just the blue sensors is shown as blue curve. We assume that these sensors measure the signal with no attenuation or distortion.

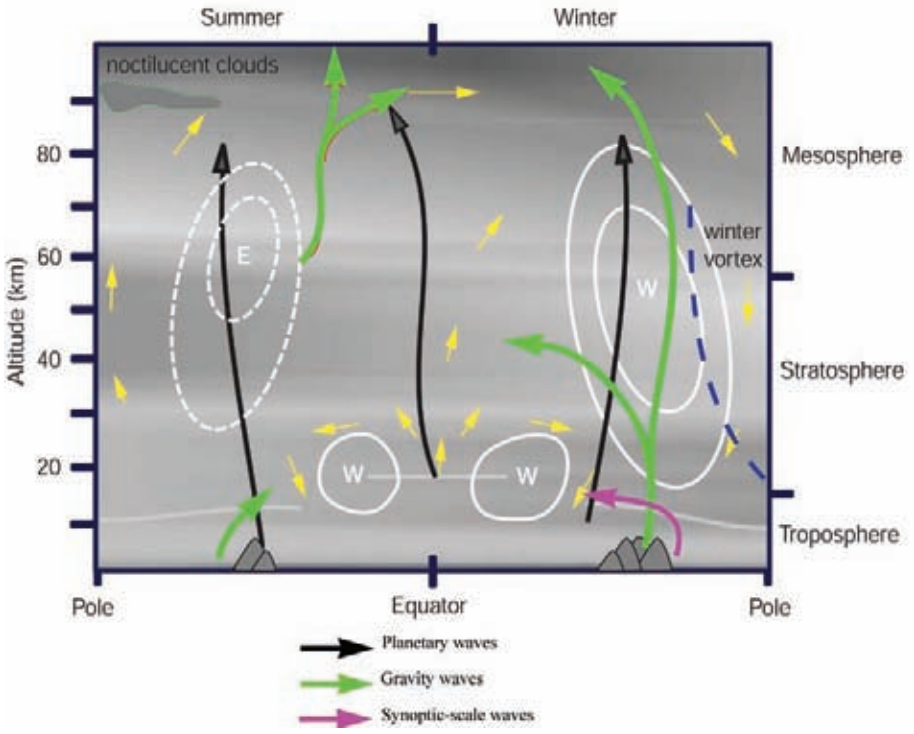

Figure 15

A schematic diagram of the atmospheric circulation and wave activities. Black, green, and magenta arrows show the energy propagation of planetary waves, gravity waves, and synoptic-scale waves, respectively. The white contours show the circumpolar flow (solid indicating west-to-east direction; dash indicating east-to-west direction). The edge of the winter Polar Vortex is shown in dash blue line. The yellow arrows indicate the slow overturning motion of the atmosphere that transports chemical species and air parcels. Adopted from the original drawing of Dr. Mark Schoberl at NASA Goddard.

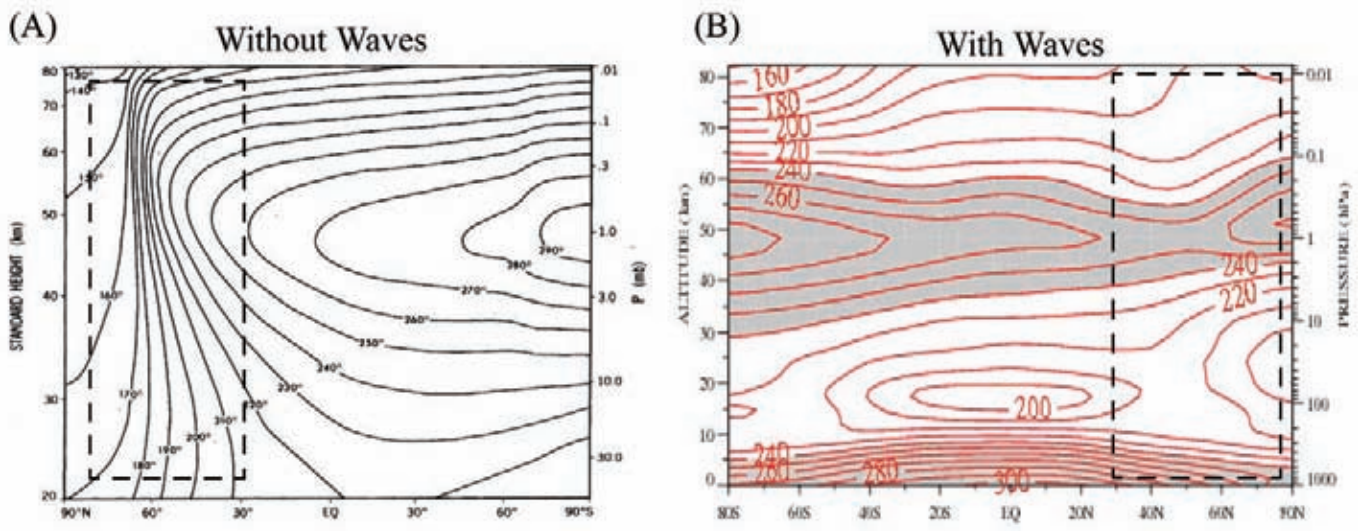

Figure 16

The effects of atmosphere waves on the climatological temperature field in January. (A) The temperature field based on radiatively determined calculation of *Fels* [1985] with no wave motion. (B) The observed temperature field from GEOS-5 analyses. The dashed box highlights the Northern Hemisphere winter region, common in both plots.

About the Author

Varavut "Var" Limpasuvan is a full professor in the Department of Chemistry and Applied Physics at Coastal Carolina University. By training, Var is a physics teacher with interests in the dynamics of Earth's atmosphere. During his first year at Coastal Carolina University (2000), he was recognized as the *Professor of the Year* by the student body. In 2007, he received the South Carolina Governor's *Young Scientist Award for Scientific Excellence*. To date, he has authored more than 20 peer-reviewed publications on atmospheric disturbances and their roles in altering large-scale flows. Married to Lourdes Limpasuvan, Var has two children: Ty and Drew. In his spare time, he enjoys traveling and seeing the world with his family. He is an avid tennis player and golfer.

Acknowledgements

This work was supported in part by the Large Scale Dynamics Program at the National Science Foundation (NSF ATM-0646672) and the National Aeronautics and Space Administration (NASA Contract NNX07AR25G). I thank Professor Louis Keiner and Dean Michael Roberts at Coastal Carolina University for supporting my award application. I am grateful for Dr. Yvan J. Orsolini at the Norwegian Institute of Air Research, Dr. Dong Wu at NASA Jet Propulsion Laboratory, and mostly my wife (Lourdes) for providing encouragements and patience during the writing of this manuscript. The editing efforts of Susan Talbot and Doug Bell are also greatly appreciated. Finally, I express sincere gratitude to Horry Telephone Cooperative (HTC) for funding the *Distinguished Teacher-Scholar Lecturer Series*.

References

- Afanasyva, Y.D. and W.R. Peltier, 2001: Numerical Simulations of Internal Gravity Wave Breaking in the Middle Atmosphere: The Influence of Dispersion and Three-Dimensionalization, *Journal of Atmospheric Sciences*, **58**, 132-153.
- Alexander, M.J., 1998: Interpretations of observed climatological patterns in stratospheric gravity wave variance, *Journal of Geophysical Research*, **103**, 8627-8640.
- Andrews, D.G., J.R. Holton, and C.B. Leovy, 1987: *Middle Atmosphere Dynamics*, Academic Press, 490 pp.
- Baldwin, M.P. and T.J. Dunkerton, 2001: Stratospheric harbingers of anomalous weather regimes, *Science*, **294**, 581-584.
- Bloom, S., A. da Silva, D. Dee, M. Bosilovich, J.D. Chern, S. Pawson, S. Schubert, M. Sienkiewicz, I. Stajner, W.W. Tan, M.-L. Wu, 2005: Documentation and Validation of the Goddard Earth Observing System (GEOS) Data Assimilation System - Version 5, *Technical Report Series on Global Modeling and Data Assimilation*, **104606**, 26.-300.
- Charlton, A.J., L.M. Polvani, J. Perlwitz, F. Sassi. E. Manzini. K. Shibata, S. Pawson, J.E. Nielsen, and D. Rind, 2007: A New Look at Stratospheric Sudden Warming. Part II: Evaluation of Numerical Model Simulations, *Journal of Climate*, **20**, 470-488.
- Fels, S.B, 1985: Radiative-dynamical interactions in the middle atmosphere, *Advances in Geophysics*, **28**A, 277.
- Fritts, D.C., and M.J. Alexander, 2003: Gravity wave dynamics and effects in the middle atmosphere, *Reviews of Geophysics,* **41**(1), 1003, doi:10.1029/2001RG000106.
- Gillett, N.P., T.D. Kell, and P.D. Jones, 2006: Regional climate impacts of the Southern Annular Mode, *Geophysical Research Letters*, **33**(23), L23704, doi:10.1029/2006GL027721.
- Hamilton, K, 2008: Numerical Resolution and Modeling of the Global Atmospheric Circulation: A Review of Our Current Understanding and Outstanding Issues, *High Resolution Numerical Modeling of the Atmosphere and Ocean*, Springer Publishing. pp. 8-27. doi10.1007/978-0387-49791-4_1.
- Hamilton, K., Y. Takahashi, and W. Ohfuchi, 2008: The Mesoscale Spectrum of Atmospheric Motions Investigated in a Very Fine Resolution Global General Circulation Model, *Journal of Geophysical Research*, **113**, D18110, doi:10.1029/2008JD009785.
- Hartmann, D.L, 1994: *Global Physical Climatology*, Academic Press, San Diego, 408 pp.
- Hartmann, D.L., J.M. Wallace, V. Limpasuvan, D.W.J. Thompson, and J.R. Holton, 2000: Can ozone depletion and global warming interact to produce rapid climate change?, *Proceedings of the National Academy of Sciences*, **97**, 1412-1417.
- Hartmann, D.L. and V. Limpasuvan, 2004: The stratosphere in the climate system, Stratospheric Processes and their Role in Climate (SPARC), *World Climate Research Programme*, **22**, January 2004.
- Holton, J.R., 1972: *An Introduction to Dynamic Meteorology*. Academic Press, New York, 319 pp.
- Hurrell, J.W, Y. Kushnir, G. Ottersen, and M. Visbeck (editors), 2003: The North Atlantic Oscillation: Climate Significance and Environmental Impact, *American Geophysical Union*, 279 pp.
- IPCC, 2001: Climate Change 2001: The Scientific Basis. Contribution of Working Group I to the Third Assessment Report of the Intergovernmental Panel on Climate Change [Houghton, J.T., Y. Ding, D.J. Griggs, M. Noguer, P.J. van der Linden, X. Dai, K. Maskell, and C.A. Johnson (eds.)]. *Cambridge University Press*, Cambridge, United Kingdom and New York, NY, USA, 881pp.
- James, I.N., 1994: *Introduction to Circulating Atmospheres*, Cambridge University Press, 422 pp.
- Kalnay E., M. Kanamitsu, R. Kistler, W. Collins, D. Deaven, L. Gandin, M. Iredell, S. Saha, G. White, J. Woollen, Y. Zhu, A. Leetmaa, R. Reynolds, M. Chelliah, W. Ebisuzaki, W. Higgins, J. Janowiak, K.C. Mo, C. Ropelewski,

- J. Wang, R. Jenne, and D. Joseph, 1996: The NCEP/NCAR 40-year reanalysis project, *Bulletin of the American Meteorological Society*, **77**, 437-470.
- Limpasuvan, V., D.L. Wu, M. Joan Alexander, M. Xue, M. Hu, S. Pawson, and J.R. Perkins, 2007:, Stratospheric gravity wave simulation over Greenland during 24 January 2005, *Journal of Geophysical Research*, **112**, D10115, doi:10.1029/2006JD007823.
- Limpasuvan, V., D.L. Hartmann, D.W.J. Thompson, K. Jeev, and Y.L. Yung, 2005: Stratosphere-troposphere evolution during polar vortex intensification, *Journal of Geophysical Research - Atmospheres*, 110, D24101, doi:10.1029/2005JD006302.
- Limpasuvan, V., D.W.J. Thompson, and D.L. Hartmann, 2004: The life cycle of Northern Hemisphere sudden stratospheric warmings, *Journal of Climate*, 17, 2584-2596.
- Limpasuvan, V. and D.L. Hartmann, 2000: Wave-maintained annular modes of climate variability, *Journal of Climate*, **13**, 4414-4429.
- Lindzen, R.S., 1981: Turbulence and stress owing to gravity wave and tidal breakdown, *Journal Geophysical Research*, **86**, 9707-9714.
- Nappo, C., 2002: *An Introduction to Atmospheric Gravity Waves*, Elsevier Press, 275 pp.
- Orsolini, Y.J. and V. Limpasuvan, 2001: The North Atlantic Oscillation and the occurrence of ozone mini-holes, *Geophysical Research Letters*, **20**, 4099-4102.
- Richter, J.H., F. Sassi, and R.R. Garcia, 2010: Towards a physically based gravity wave source parameterization, *Journal of Geophysical Research*, in press.
- Salby, M.L., 1996: Fundamentals of Atmospheric Physics, Volume 61 (International Geophysics), *Academic Press*, 624 pp.
- Siskind, D.E., S.D. Eckermann, L. Coy, and J.P. McCormack, 2007: On recent interannual variability of the Arctic winter mesosphere: Implications for tracer descent, *Geophysical Research Letters*, **43**, L09806, doi:10.1029/2007GL029293.
- Schwartz, M.J., W.G. Read, W.V. Snyder, 2006: Polarized radiative transfer for Zeeman-split oxygen lines in the EOS MLS forward model. IEEE *Trans. Geosci. Remote Sensing*, **44** (5), 1182–1191.
- Thompson, D.W.J, and J.M. Wallace, 1998: The Arctic Oscillation signature in the wintertime geopotential height and temperature fields, *Geophysical Research Letters*, **25**, 1297-1300.
- Thompson, D.W.J., and J.M. Wallace, 2001: Regional Climate Impacts of the Northern Hemisphere Annular Mode, *Science*, **293**, 85-89
- Waters, J.W., L. Froidevaux, R.S. Harwood, et al., 2006 The Earth Observing System Microwave Limb Sounder (EOS MLS) on the Aura satellite. IEEE *Trans. Geosci. Remote Sensing*, **44** (5), 1075–1082.
- Wallace, J.M and P. Hobbs: 2006: Atmospheric Science, Volume 92, Second Edition: An Introductory Survey (International Geophysics), A*cademic Press*, 483 pp.
- Wu, D.L., 2004: Mesoscale Gravity Wave Variances from AMSU-A Radiances, *Geophysical Research Letters*, **28**, No. 12, doi: 10.1029/ 2004GL019562.
- Xue, M., D. Wang, J. Gao, and K.K. Droegemeier, 2003: The Advanced Regional Prediction System (ARPS), storm-scale numerical weather predication and data assimilation, *Meteorology and Atmospheric Physics*, **82**, 130–170, doi:10.1007/s00703-001-0595-6.

The Distinguished Teacher-Scholar Lecturer Series is made possible through the generous support of Horry Telephone Cooperative, Inc.

Coastal Carolina University
P.O. Box 261954 • Conway, South Carolina 29528-6054
www.coastal.edu